Constraining new physics in entangled two-qubit systems: top-quark, tau-lepton and photon pairs

M. Fabbrichesi[†], R. Floreanini[†], and E. Gabrielli[‡†*]
[†] *INFN, Sezione di Trieste, Via Valerio 2, 34127 Trieste, Italy*
[‡] *Physics Department, University of Trieste, Strada Costiera 11, 34151 Trieste, Italy and*
[*] *Laboratory of High-Energy and Computational Physics, NICPB, Ravala 10, 10143 Tallinn, Estonia*

(Dated: March 28, 2023)

The measurement of quantum entanglement can provide a new and most sensitive probe to physics beyond the Standard Model. We use the concurrence of the top-quark pair spin states produced at colliders to constrain the magnetic dipole term in the coupling between top quark and gluons, that of τ-lepton pairs spin states to bound contact interactions and that of τ-lepton pairs or two-photons spin states from the decay of the Higgs boson in trying to distinguish between CP-even and odd couplings. These four examples show the power of the new approach as well as its limitations. We show that differences in the entanglement in the top-quark and τ-lepton pair production cross sections can provide constraints better than those previously estimated from total cross sections or classical correlations. Instead, the final states in the decays of the Higgs boson remain maximally entangled even in the presence of CP-odd couplings and cannot be used to set bounds on new physics. We discuss the violation of Bell inequalities featured in all four processes.

arXiv:2208.11723v2 [hep-ph] 26 Mar 2023

I. ENTANGLEMENT AT WORK IN HIGH-ENERGY PHYSICS

Collider physics is all about the production of particles from the interaction and the decay of other particles. Consider the case of the production of just two of these particles: We can study their momenta, energies and spin to reconstruct their properties and compare them to those expected in the Standard Model (SM)—or in an extension of it. The same observables of the system of two particles partake in correlations that are proper of their quantum state and that give rise to the very characteristic property of *entanglement* (for a review, see [1]). Because they are entangled, the two particles share properties—most notably, their spin correlations—that can only be discussed in the system as a whole.

Though a preeminent feature in atomic physics, quantum correlations among the components of a system has been somewhat played down in quantum field theory because of the fixed momentum representation of the states in Fock space and the commuting nature of the momentum and occupation number variables. Nevertheless, the quantum nature of the particles produced in high-energy collisions is there and their study could lead to new insights into their interaction.

Probing entanglement at collider was first proposed in [2, 3]. Tests in the high-energy regime of particle physics have been suggested by means of neutral meson physics [4, 5], Positronium [6], Charmonium decays [7] and neutrino oscillations [8]. A discussion of some of these issues also appears in [9, 10].

The interest has been revived recently after entanglement has been shown [11] to be present in top-quark pair production at the LHC and it was argued [12] that Bell inequalities violation is experimentally accessible in the same system. Following this lead, there has been more work about top-quark production [13–16], hyperons [17] and gauge bosons from Higgs boson decay [18, 19]. For all these particles, it is possible to study entanglement and verify the violation of Bell inequalities.

The same framework suggests the possibility of studying what happens when the SM amplitudes are modified by introducing new physics beyond the SM. Because of its being so very fragile, entanglement provides a very sensitive probe to possible new physics in those cases where the SM states are produced in an entangled state which the new physics tends to lessen, modify or brake altogether. In general, by adding extra terms to the SM interactions, the entanglement of the states is modified and the amount of change is a sensitive function of the new physics present—which allows for direct constraints to be set.

A first study of the impact of effective operators of dimension six—within the SM Effective Field Theory (SMEFT)—has been presented in [20] for the entanglement of the spins of top-quark pairs. In this work we want to provide a comprehensive discussion for the case of bipartite, two-qubit like systems available at colliders and explore to what extent entanglement can provide a new tool in the search of physics beyond the SM.

We find that entanglement provides a novel set of observables that could lead to improved constraints with respect to those extracted from total cross sections or classical correlations. Quantum correlations can readily be studied in a bipartite system made of either two spin-1/2 particles or two massless spin-1 (photons) [21]. Polarizations are measured at colliders only for heavy fermions, the decays of which act as their own polarimeters; for this reason, we study in detail the system of top-quark and τ-lepton pairs produced at colliders. For the τ-lepton pairs we also discuss

the case of their coming from the decay of the Higgs boson. In addition, we include the case of the decay of the Higgs boson into two photons because it can be modeled as a two-qubit system too and the framework is analogous to that of two fermions. We model the new physics by considering the effect of representative operators not present within the SM and use the entanglement observables to constrain the size of their contribution.

For all these four systems we also check the Bell inequalities and find that they are maximally violated in the case of the Higgs boson decays.

New analytical results for the polarization matrix of the Drell-Yan processes $q\bar{q} \to \tau\bar{\tau}$ in the SM and beyond, as well as the Higgs decay into $\tau^+\tau^-$ and into two photons, are provided in the Appendix, which also includes known analytical results for the top-quark pair production $q\bar{q} \to t\bar{t}$.

II. METHODS

The quantum state of a bipartite system that can be modeled as a two-qubit pair, can be represented by the following Hermitian, normalized, 4×4 density matrix:

$$\rho = \frac{1}{4}\Big[\mathbb{1}\otimes\mathbb{1} + \sum_i B_i^+(\sigma_i\otimes\mathbb{1}) + \sum_j B_j^-(\mathbb{1}\otimes\sigma_j) + \sum_{ij} C_{ij}(\sigma_i\otimes\sigma_j)\Big]\,, \tag{1}$$

where σ_i are Pauli matrices, $\mathbb{1}$ is the unit 2×2 matrix, while the sums of the indices i, j run over the labels representing any orthonormal reference frame in three-dimensions.

The real coefficients $B_i^+ = \mathrm{Tr}[\rho\,(\sigma_i\otimes\mathbb{1})]$ and $B_j^- = \mathrm{Tr}[\rho\,(\mathbb{1}\otimes\sigma_j)]$ represent the polarization of the two qubits, while the real matrix $C_{ij} = \mathrm{Tr}[\rho\,(\sigma_i\otimes\sigma_j)]$ gives their correlations. In the case of the particle pair system, $B_i^\pm$ and C_{ij} are functions of the parameters describing the kinematics of the pair production. In addition, these coefficients need to satisfy further constraints coming from the positivity request, $\rho \geq 0$, that any density matrix should fulfill; these extra conditions are in general non-trivial, as they originate from requiring all principal minors of the matrix ρ to be non-negative.

The two-qubit state ρ is separable if it can be expressed as a convex combination of two-qubit product states:

$$\rho = \sum_{ij} p_{ij}\,\rho_i^{(1)}\otimes\rho_j^{(2)}\,, \quad \text{with} \quad p_{ij} > 0 \quad \text{and} \quad \sum_{ij} p_{ij} = 1\,, \tag{2}$$

where $\rho_i^{(1)}$ and $\rho_j^{(2)}$ are single-qubit density matrices. All states ρ that can not be written in the form of Eq. (2) are called entangled and exhibit quantum correlations.

Correlations along only one direction in a given frame of reference can only probe classical properties as in the case of angular momentum conservation—the correlation in this case being that if, say, spin up for one particle is measured in the direction z, necessarily spin down will be measured in the same direction for the other particle, assuming the initial state has spin zero. It is only by the simultaneous measurement of correlations along more axes (or different bases) that we can probe quantum correlations, in particular, by measuring non-commuting quantities for the two particles, as in the case of the spin along the z direction for the first particle and the spin along the x direction for the second one. This is the reason why the full matrix C_{ij} is required in the study of entanglement.

Quantifying the entanglement content of a quantum state is in general a hard problem, but for bipartite systems made of two qubits, an easily computable measure is available, the *concurrence* [22]. It is constructed using the auxiliary 4×4 matrix

$$R = \rho\,(\sigma_2\otimes\sigma_2)\,\rho^*\,(\sigma_2\otimes\sigma_2)\,, \tag{3}$$

where ρ^* denotes the matrix with complex conjugated entries. Although non-Hermitian, the matrix R possesses non-negative eigenvalues; denoting with λ_i, $i = 1, 2, 3, 4$, their square roots and assuming λ_1 to be the largest, the concurrence of the state ρ is defined as

$$\mathcal{C}[\rho] = \max\left(0, \lambda_1 - \lambda_2 - \lambda_3 - \lambda_4\right)\,. \tag{4}$$

Concurrence vanishes for separable states, like those defined in (2), reaching its maximum value 1 when ρ is a projection on a pure, maximally entangled state.

The presence of entanglement in a quantum system, that is of correlations among its constituents not accounted for by classical physics, can lead to the violation of suitable constraints, the so-called Bell inequalities, that are instead satisfied by certain local, stochastic completions of quantum mechanics [21, 23, 24]. In the case of a two-qubit system

in the state (1), as a pair of spin-1/2 particles, a very useful test is provided by the the following inequality involving only the correlation matrix C [25]:

$$\left|\hat{n}_1 \cdot C \cdot \left(\hat{n}_2 - \hat{n}_4\right) + \hat{n}_3 \cdot C \cdot \left(\hat{n}_2 + \hat{n}_4\right)\right| \leq 2 \,, \tag{5}$$

where $\hat{n}_1$, $\hat{n}_2$, $\hat{n}_3$ and $\hat{n}_4$ are four different three-dimensional unit vectors determining four spatial directions, along which the spins of the two particles can be measured. In order to test this (generalized) Bell inequality one needs to maximize the left-hand side of (5) by a suitable choice of the four spatial directions. In practice, this maximization procedure can be overcome by looking at the eigenvalues m_1, m_2, m_3, of the symmetric, non-negative, 3×3 matrix $M = C^T C$, where C^T is the transpose of C, that can be ordered in decreasing magnitude $m_1 \geq m_2 \geq m_3$. At this purpose it is convenient to introduce the operator $\mathfrak{m}_{12}[C]$ defined as

$$\mathfrak{m}_{12}[C] \equiv m_1 + m_2 \,. \tag{6}$$

As proven in [25], given a two-qubit state ρ as in (1), with a correlation matrix C satisfying the condition

$$\mathfrak{m}_{12}[C] > 1 \,. \tag{7}$$

then there surely are choices for the vectors $\hat{n}_1$, $\hat{n}_2$, $\hat{n}_3$, $\hat{n}_4$ for which the left-hand side of (5) is larger than 2; in other words, the two-qubit state (1) violates (5) if and only if the sum of the two largest eigenvalues of M is strictly larger than 1.

In the following we concentrate on the two observables:

$$\mathcal{C}[\rho] \quad \text{and} \quad \mathfrak{m}_{12}[C] \,. \tag{8}$$

We use the first to constrain possible new physics extension of the SM by studying spin correlations in top-quark and τ-lepton pairs produced at colliders, the second to check violations of the Bell inequalities in the same pair systems as well as in the decay of the Higgs boson into τ-lepton pairs and two photons.

Although other entanglement witnesses have been considered in high-energy physics [11, 20], we stress that the concurrence $\mathcal{C}[\rho]$ directly and fully quantifies the entanglement content of the state ρ, it can be easily computed and readily measured in experiments. The observable $\mathfrak{m}_{12}[C]$ witnesses Bell non-locality and thus it is perfectly suited to test the Bell inequality (5); indeed, as already remarked, it automatically selects the best choice of the four units vectors $\hat{n}_i$ that maximizes the left-hand side of (5) and thus its violation.

1. *Kinematics and projector operators*

We consider the cross section for the process in which two parton quarks go into two final fermions

$$q(q_1) + \bar{q}(q_2) \to f(k_1) + \bar{f}(k_2) \,. \tag{9}$$

The momenta k_1 and k_2 of the final fermion and anti-fermion, and q_1 and q_2 of the entering quark and anti-quark, respectively, can be written in the center-of-mass (CM) system as

$$\begin{aligned}
k_1 &= \left(\frac{m_f}{\sqrt{1-\beta_f^2}},\, \frac{m_f \beta_f \sin\Theta}{\sqrt{1-\beta_f^2}},\, 0,\, \frac{m_f \beta_f \cos\Theta}{\sqrt{1-\beta_f^2}}\right) \\
k_2 &= \left(\frac{m_f}{\sqrt{1-\beta_f^2}},\, -\frac{m_f \beta_f \sin\Theta}{\sqrt{1-\beta_f^2}},\, 0,\, -\frac{m_f \beta_f \cos\Theta}{\sqrt{1-\beta_f^2}}\right) \\
q_1 &= \left(\frac{m_f}{\sqrt{1-\beta_f^2}},\, 0,\, 0,\, \frac{m_f}{\sqrt{1-\beta_f^2}}\right) \\
q_2 &= \left(\frac{m_f}{\sqrt{1-\beta_f^2}},\, 0,\, 0,\, -\frac{m_f}{\sqrt{1-\beta_f^2}}\right) \,,
\end{aligned} \tag{10}$$

where m_f is the mass of the final fermions and

$$\beta_f = \sqrt{1 - 4\frac{m_f^2}{m_{f\bar{f}}^2}}\,, \tag{11}$$

where $m_{f\bar{f}}$ is the fermion-pair invariant mass, with Θ the angle between the initial and final fermion momenta in the CM frame.

Spin correlations, as embodied by the coefficients C_{ij} in Eq. (1), are extracted from the cross section by taking the product of the polarizations of the final fermions. This is done by means of the usual projectors over definite polarizations (for a fermion with momentum p, mass m_f and polarization vector ζ):

$$u(p,\zeta)\otimes\bar{u}(p,\zeta) = \frac{1}{2}(\not{p} + m_f)(1 - \gamma_5\not{\zeta}) \quad \text{and} \quad v(p,\zeta)\otimes\bar{v}(p,\zeta) = \frac{1}{2}(\not{p} - m_f)(1 - \gamma_5\not{\zeta})\,, \tag{12}$$

inserted in the square of the modulus of the amplitude. The coefficients $B_i^{\pm}$ in Eq. (1) are instead obtained by keeping only one of the two particle polarizations.

We adopt the orthonormal basis introduced in [26] in order to describe the spin correlations thus obtained. Let $\hat{p}$ the unit vector along one of the proton beam directions in the laboratory frame and denote with $\hat{k}$ the direction of flight of the final fermion in the fermion pair CM frame; then, a convenient reference frame is defined by the three unit vectors:

$$\hat{r} = \frac{1}{r}(\hat{p} - y\hat{k})\ , \qquad \hat{n} = \frac{1}{r}(\hat{p}\times\hat{k})\ , \tag{13}$$

where

$$y = \hat{p}\cdot\hat{k} = \cos\Theta\ , \qquad r = \sqrt{1-y^2}\ , \tag{14}$$

with Θ being the scattering angle. Notice, that at partonic level the angle Θ is defined, according to the momenta in Eq. (10), as the angle between initial quarks and final fermion.

The elements C_{ij} of the correlation matrix in Eq. (1) are obtained on the various components of the chosen basis by means of the polarizations vectors:

$$\begin{aligned}
\zeta_1^k &= \left(\frac{\beta_f}{\sqrt{1-\beta_f^2}},\ \frac{\sin\Theta}{\sqrt{1-\beta_f^2}},\ 0,\ \frac{\cos\Theta}{\sqrt{1-\beta_f^2}}\right)\\
\zeta_2^k &= \left(-\frac{\beta_f}{\sqrt{1-\beta_f^2}},\ \frac{\sin\Theta}{\sqrt{1-\beta_f^2}},\ 0,\ \frac{\cos\Theta}{\sqrt{1-\beta_f^2}}\right)\\
\zeta_1^r &= \zeta_2^r = (0,\ -\cos\Theta,\ 0,\ \sin\Theta)\\
\zeta_1^n &= \zeta_2^n = (0,\ 0,\ 1,\ 0)
\end{aligned} \tag{15}$$

where the indices 1 and 2 stand for the final fermion and anti-fermion.

The differential cross section for pair $f\bar{f}$ production is given by

$$\frac{\mathrm{d}\sigma^{f\bar{f}}}{\mathrm{d}\Omega} = \frac{\beta_f\,|\overline{\mathcal{M}}|^2}{64\pi^2\,m_{f\bar{f}}^2}\,, \tag{16}$$

where $\mathcal{M}$ is the amplitude for the production and β_f is defined in Eq. (11).

The parton level differential cross section for the two partons—with fraction x_1 and x_2 of the available momentum and momentum distribution (PDF) $q(x)$ and $\bar{q}(x)$—is given by

$$\frac{\mathrm{d}\sigma^{f\bar{f}}}{\mathrm{d}\Omega\,\mathrm{d}m_{f\bar{f}}} = 2\int\frac{\mathrm{d}\sigma^{f\bar{f}}}{\mathrm{d}\Omega}q(x_1)\bar{q}(x_2)\delta(m_{f\bar{f}}^2 - x_1x_2s)\,\mathrm{d}x_1\mathrm{d}x_2\,, \tag{17}$$

for CM energy $\sqrt{s}$. The cross section in Eq. (17) can be re-written in terms of the parton luminosity function

$$L^{q\bar{q}}(\tau) = \frac{4\tau}{\sqrt{s}}\int_\tau^{1/\tau}\frac{\mathrm{d}z}{z}q_q(\tau z)q_{\bar{q}}\left(\frac{\tau}{z}\right) \tag{18}$$

by the change of variables $x_1 = \tau/z$ and $x_2 = \tau z$, with $m^2_{f\bar{f}} = \tau^2 s$. In Eq. (18) there is an overall factor 2 due to the symmetrization between quark and anti-quark. We use the parton luminosity function in Eq. (18), as well as the corresponding one for the case of having gluons as the partons, in what follows. The differential cross section in Eq. (17) can thus be written as

$$\frac{\mathrm{d}\sigma^{f\bar{f}}}{\mathrm{d}\Omega\,\mathrm{d}m_{f\bar{f}}} = \frac{\beta_f\,|\overline{\mathcal{M}}|^2}{64\pi^2\,m^2_{f\bar{f}}} L^{q\bar{q}}(\tau)\,, \tag{19}$$

where $L^{q\bar{q}}(\tau)$ stands for the luminosity functions of the corresponding quark or gluon partons.

In the case of the Higgs boson H decay

$$H \to f(k_1)\bar{f}(k_2)\,, \tag{20}$$

the same four-vectors in Eq. (10) can be used by imposing $m_{f\bar{f}} = m_h$ and putting q_1 and q_2 at rest and equal; the vectors k_1 and k_2 are back-to-back with no scattering angle dependence. The polarization of the final states follows the same structure as given in Eq. (12), with polarization vectors as in Eq. (15). The corresponding C_{ij} elements are obtained in the same way as above, by projecting on the various components of the chosen basis for the polarization vectors in Eq. (15).

Regarding the Higgs boson decay into two photons

$$H \to \gamma(k_1)\,\gamma(k_2)\,, \tag{21}$$

the projection in the product of the associated two photon polarizations $e^{\lambda_1}_\mu(k_1)$ and $e^{\lambda_2}_\mu(k_2)$ (with both λ_1 and λ_2 indices taking values 1 and 2) can be obtained in similar fashion by expressing the corresponding density matrix $\rho_{\mu\nu}$ for a photon of generic momentum k and polarization $e^{\lambda_1}_\mu(k)$ as a function of the Stokes parameters ξ_i :

$$\begin{aligned}\rho_{\mu\nu}(\vec{\xi}) = e^{\lambda}_\mu(k) e^{\lambda'*}_\nu(k) \;&=\; \frac{1}{2}\hat{e}^T_\mu\Big(\mathbb{1} + \vec{\xi}\cdot\vec{\sigma}\Big)\hat{e}_\nu \\ &= \frac{1}{2}\Big(e^{(1)}_\mu e^{(1)}_\nu + e^{(2)}_\mu e^{(2)}_\nu\Big) + \frac{\xi_1}{2}\Big(e^{(1)}_\mu e^{(2)}_\nu + e^{(2)}_\mu e^{(1)}_\nu\Big) \\ &\quad -\frac{i\xi_2}{2}\Big(e^{(1)}_\mu e^{(2)}_\nu - e^{(2)}_\mu e^{(1)}_\nu\Big) + \frac{\xi_3}{2}\Big(e^{(1)}_\mu e^{(1)}_\nu - e^{(2)}_\mu e^{(2)}_\nu\Big)\,,\end{aligned} \tag{22}$$

where the compact vectorial notation $\hat{e}_\mu \equiv (e^{(1)}_\mu, e^{(2)}_\mu)$ is adopted, with $\hat{e}^T_\mu$ standing for the transpose, k the photon 4-momentum, and σ_i the Pauli matrices; the four-vectors $e^{(\lambda)}_\mu$ provide a basis for the linear polarizations, they are two ortho-normal four-vectors orthogonal to the momentum: $e^{(\lambda)}\cdot e^{(\lambda')} = -\delta^{\lambda\,\lambda'}$, $e^{(\lambda)}_\mu \cdot k = 0$. To lighten the notation, we removed the momentum dependence inside the polarization basis.

For the two photon system, the product $\rho(\vec{\xi}^{(1)})\rho(\vec{\xi}^{(2)})$ of the two density matrix enters, with $\vec{\xi}^{(1)}, \vec{\xi}^{(2)}$ the corresponding Stokes parameters of the two photons. In this case the correlation matrix C_{ij} for the two photon system is expressed on the basis of the Stokes parameters and it can be simply extracted by selecting the terms proportional to $\xi^{(1)}_i \xi^{(2)}_j$ in the expression for the polarized amplitude square $|\mathcal{M}^2|$ of the process, and dividing them for the unpolarized $|\bar{\mathcal{M}}^2|$ contribution. Analogously, for the B^+_i or B^-_i terms in Eq. (1), which can be extracted taking the linear terms proportional to the corresponding Stokes parameters $\xi^{(1)}_i$ or $\xi^{(2)}_i$ respectively, in the expression of $|\mathcal{M}^2|$ and normalizing them by $|\bar{\mathcal{M}}^2|$.

2. *Uncertainty estimates*

The setting of bounds on physics beyond the SM is all about the knowing the uncertainty of our limits. To estimate the intrinsic uncertainty in the determination of observables in Eq. (8) for the various processes we are going to consider, we run 1000 pseudo-experiments according to the probability distribution of the observables themselves.

For example, in comparing SM and new physics, from the distributions of the observable value in the scattering angle and the invariant mass obtained for the two cases, we can obtain the significance with which we can separate the two. To quantify this difference in terms of statistical significance, we compute the p-value of the new physics distribution by integrating the SM distribution from the mean value to $-\infty$.

The significance is defined as $\mathcal{Z} = \Phi^{-1}(1-p)$ where

$$\Phi(x) = \frac{1}{2}\left[1 + \mathrm{erf}\left(\frac{x}{\sqrt{2}}\right)\right]\,. \tag{23}$$

The value of $\mathcal{Z}$ assigns a statistical significance to the separation between the two distributions. We can take $\mathcal{Z}$ as the number of standard deviations σ, in the approximation in which the distribution is assumed to be Gaussian, and translates the number of standard deviations into a confidence level (CL).

In the case of the Higgs boson decays, since there is no kinematical variation, we simply draw a Gaussian dispersion with $\sigma = 1/\sqrt{N}$, where N is taken from the corresponding number of events generated by the production cross sections and branching ratios multiplied for the benchmark luminosities. In those cases for which this number is very large, we simply take 1000 events as an illustrative example.

As we comment further for the specific examples, all these estimates of uncertainty are limited by being performed at the level of primary parton production. They do not take into account the additional uncertainty coming from the extraction of the entanglement observables from the actual data—which are the angular distributions of the final states originating from the decays of the top quarks and τ-leptons. As shown in [12] for the case of the top quark pairs, we do expect a substantial additional uncertainty from systematic errors in the reconstruction. In addition, there may also be other confounding contributions from possible background events.

III. RESULTS: TOP QUARK PAIRS

Top quark pairs are routinely produced at the LHC and the spin correlations among quark pairs has been shown [27–31] to be a powerful tool in the physical analysis—limited aspects of which have been already studied by the experimental collaborations at the LHC on data at 7 [32], 8 [33] and 13 TeV [34] of CM energy.

In this section we study the operators in Eq. (8) in the case of top-quark pairs and use them to constrain new physics and check the Bell inequalities.

A. Entanglement in $t\bar{t}$ production

Before plunging into the actual analysis of spin correlations in the top-quark pair production, it is useful to discuss qualitatively what the SM predicts for the entanglement content of the $t\bar{t}$-spin state as described by a density matrix $\rho_{t\bar{t}}$ as in (1).

The dependence of the entries of the matrix (1) on the kinematic variables Θ, the scattering angle, and β_t, as defined in Eq. (11), is in general rather involved but it simplifies at $\Theta = \pi/2$ for which the top-quark pair is transversally produced and the entanglement is maximal. In this limit, we choose the three vectors $\{\hat{r},\, \hat{k},\, \hat{n}\}$ to point in the $\{\hat{x}, \hat{y}, \hat{z}\}$ directions. In this frame, let us denote by $|0\rangle$ and $|1\rangle$ the eigenvectors of the Pauli matrix σ_z with eigenvalues -1 and $+1$, respectively; similarly, let $|-\rangle$ and $|+\rangle$ be the analogous eigenvectors of σ_x and $|\mathrm{L}\rangle$ and $|\mathrm{R}\rangle$ those of σ_y.

Possible quark pair spin density matrices can be both projectors on pure, maximally entangled Bell states,

$$\rho^{(\pm)} = |\psi^{(\pm)}\rangle\langle\psi^{(\pm)}| \,, \qquad |\psi^{(\pm)}\rangle = \frac{1}{\sqrt{2}}\big(|01\rangle \pm |10\rangle\big) \,, \tag{24}$$

and mixed, unentangled states,

$$\rho^{(1)}_{\rm mix} = \frac{1}{2}\Big(|{+}{+}\rangle\langle{+}{+}| + |{-}{-}\rangle\langle{-}{-}|\Big) \,, \tag{25}$$

$$\rho^{(2)}_{\rm mix} = \frac{1}{2}\Big(|\mathrm{LR}\rangle\langle\mathrm{LR}| + |\mathrm{RL}\rangle\langle\mathrm{RL}|\Big) \,, \tag{26}$$

$$\rho^{(3)}_{\rm mix} = \frac{1}{2}\Big(|01\rangle\langle 01| + |10\rangle\langle 10|\Big) \,. \tag{27}$$

Let us treat separately the quark-antiquark $q\bar{q}$ and gluon-gluon gg production channels. For the $q\bar{q}$ production channel, using the explicit expression collected in the Appendix for the correlation coefficients C_{ij}, one obtains that the $t\bar{t}$ spin density matrix can be expressed as the following convex combination:

$$\rho^{(q\bar{q})}_{t\bar{t}} = \lambda\rho^{(+)} + (1-\lambda)\rho^{(1)}_{\rm mix} \,, \quad \text{with} \quad \lambda = \frac{\beta_t^2}{2-\beta_t^2} \in [0,1] \,, \tag{28}$$

so that at high transverse momentum, $\beta_t \to 1$, the spins of the $t\bar{t}$ pair tend to be generated in a maximally entangled state; this quantum correlation is however progressively diluted for $\beta_t < 1$, vanishing at threshold, $\beta_t = 0$, as the two spin state becomes a totally mixed, separable state.

The situation is different for the gg production channel, as both at threshold and at high momentum the $t\bar{t}$ spins result maximally entangled, with $\rho^{(gg)}_{t\bar{t}} = \rho^{(+)}$ for $\beta_t \to 1$ and $\rho^{(gg)}_{t\bar{t}} = \rho^{(-)}$ when $\beta_t = 0$. For intermediate values of β_t, the situation becomes more involved, and the two-spin density matrix can be expressed as the following convex combination:

$$\rho^{(gg)}_{t\bar{t}} = a\rho^{(+)} + b\rho^{(-)} + c\rho^{(1)}_{\rm mix} + d\rho^{(2)}_{\rm mix} \,, \tag{29}$$

with non-negative coefficients

$$a = \frac{\beta_t^4}{1 + 2\beta_t^2 - 2\beta_t^4} \,, \quad b = \frac{(1-\beta_t^2)^2}{1 + 2\beta_t^2 - 2\beta_t^4} \,, \quad c = d = \frac{2\beta_t^2(1-\beta_t^2)}{1 + 2\beta_t^2 - 2\beta_t^4} \,, \tag{30}$$

so that $a + b + c + d = 1$, while entanglement is less than maximal.

Putting together the $q\bar{q}$- and gg-contributions, as discussed below, leads to more mixing and therefore in general to additional loss of quantum correlations. Nevertheless, this preliminary analysis already indicates that in order to get the larger $t\bar{t}$-pair spin entanglement one has to look at the kinematic region of high energy and large scattering angle.

B. Computing the observables

We compute all the entries of the correlation matrix C_{ij} for the process

$$p + p \to t + \bar{t} \,. \tag{31}$$

with the unpolarized cross section given by

$$\frac{{\rm d}\sigma}{{\rm d}\Omega\, {\rm d}m_{t\bar{t}}} = \frac{\alpha_s^2 \beta_t}{64\pi^2 m_{t\bar{t}}^2} \Big\{ L^{gg}(\tau)\, \tilde{A}^{gg}[m_{t\bar{t}}, \Theta] + L^{qq}(\tau)\, \tilde{A}^{qq}[m_{t\bar{t}}, \Theta] \Big\} \tag{32}$$

where $L^{gg,qq}(\tau)$ are the parton luminosity functions defined in Eq. (18) of section II, $\tau = m_{t\bar{t}}/\sqrt{s}$ and $\alpha_s = g^2/4\pi$. The explicit expressions for $\tilde{A}^{gg}$ and $\tilde{A}^{qq}$ are given in the Appendix.

The combination of the two channels (see Fig. 1) $g + g \to t + \bar{t}$ and $q + \bar{q} \to t + \bar{t}$ in Eq. (32) is weighted by the respective parton luminosity functions

$$L^{gg}(\tau) = \frac{2\tau}{\sqrt{s}} \int_\tau^{1/\tau} \frac{{\rm d}z}{z} q_g(\tau z) q_g\left(\frac{\tau}{z}\right) \quad \text{and} \quad L^{qq}(\tau) = \sum_{q=u,d,s} \frac{4\tau}{\sqrt{s}} \int_\tau^{1/\tau} \frac{{\rm d}z}{z} q_q(\tau z) q_{\bar{q}}\left(\frac{\tau}{z}\right) \,, \tag{33}$$

where the functions $q_j(x)$ are the PDFs. Their numerical values are those provided by a recent sets (PDF4LHC21) [35] for $\sqrt{s} = 13$ TeV and factorization scale $q_0 = m_{t\bar{t}}$ (we have used for all our results the subset 40).

The correlation coefficients are given as

$$C_{ij}[m_{t\bar{t}}, \Theta] = \frac{L^{gg}(\tau)\, \tilde{C}^{gg}_{ij}[m_{t\bar{t}}, \Theta] + L^{qq}(\tau)\, \tilde{C}^{qq}_{ij}[m_{t\bar{t}}, \Theta]}{L^{gg}(\tau)\, \tilde{A}^{gg}[m_{t\bar{t}}, \Theta] + L^{qq}(\tau)\, \tilde{A}^{qq}[m_{t\bar{t}}, \Theta]} \,. \tag{34}$$

The explicit expression for the coefficient $\tilde{C}^{gg}_{ij}$ and $\tilde{C}^{qq}_{ij}$ for the SM as well as for the new physics are collected in the Appendix.

The expression in Eq. (34) must be expanded in the case of new physics by retaining terms linear in the new physics coefficient. As already remarked, the combination of different terms in the cross section implies a decrease in entanglement. For this reason, the parton luminosities play an important role.

C. Bell inequalities

Let us first discuss the violation of Bell inequalities coming from the entanglement of the top-quark pair. This violation has been already discussed in [12] by means of a numerical simulation of the data of run2 at the LHC and finding an estimate of $\mathfrak{m}_{12}[C] > 1$ with a CL 95%. The estimate of the operator $\mathfrak{m}_{12}[C]$ requires a correction for the inherent bias in the numerical computation of the eigenvalues. The operator is a consistent estimator and its use in testing the violation of Bell inequalities, as in [12], valid. Such an analysis provides, as already mentioned, a more

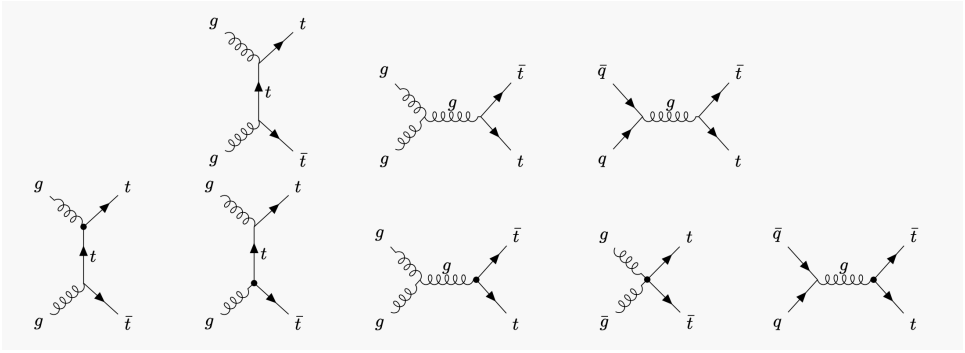


FIG. 1. Feynman diagrams for $t\bar{t}$ production. The dot stands for the magnetic dipole vertex (see Eq. (37)).

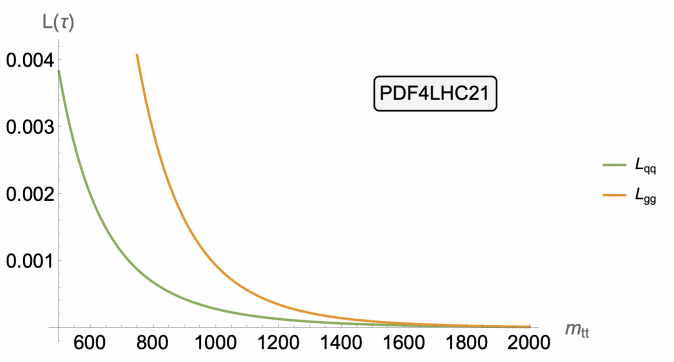


FIG. 2. Parton luminosities: The gluon luminosity is about 9 times larger than the quark luminosity at threshold, then decreasing to being about 30% larger around 1 TeV.

realistic estimate of the uncertainty than that we are going to provide here which is only based on the primary particle production.

Here we compute the violation of the Bell inequalities directly from the analytical expression of $\mathfrak{m}_{12}[C]$ in Eq. (6). Because the only off-diagonal term in the matrix

$$C = \begin{pmatrix} C_{nn} & C_{nr} & C_{nk} \\ C_{rn} & C_{rr} & C_{rk} \\ C_{kn} & C_{kr} & C_{kk} \end{pmatrix} , \tag{35}$$

is C_{kr}, its eigenvalues are given by

$$C_{nn}^2, \quad \frac{1}{4}\left[C_{kk} + C_{rr} + \sqrt{(C_{kk}^2 - C_{rr})^2 + 4C_{kr}^2}\right]^2, \quad \frac{1}{4}\left[C_{kk} + C_{rr} - \sqrt{(C_{kk}^2 - C_{rr})^2 + 4C_{kr}^2}\right]^2 . \tag{36}$$

The sum of the two largest among the three eigenvalues in Eq. (36) give us the value of the operator $\mathfrak{m}_{12}[C]$.

The values of the observable $\mathfrak{m}_{12}[C]$ across the entire kinematical space available are shown in the contour plot in Fig. 3. In this and the following contour plots the values of the observable are symmetric for $1 < 2\Theta/\pi < 2$. The figure shows how the quantum entanglement increases as we consider larger scattering angles and, as expected from the qualitative discussion in section III.A, is maximal for $m_{t\bar{t}} > 900$. Therefore, we zoom in the kinematical window where the observable $\mathfrak{m}_{12}[C]$ is larger, namely for $m_{t\bar{t}} > 900$ GeV and $2\Theta/\pi > 0.85$. The mean value of $\mathfrak{m}_{12}[C]$ in this bin is 1.44.

We give in Table I the number of events for the two benchmark cases of the run 2 LHC and the future Hi-Lumi. Cross sections are computed by running MADGRAPH5 [36] at the LO and then correcting by the κ-factor given at the NNLO [37]. These are events in which the two tops decay into leptons (BR 2.3%)

To estimate the intrinsic uncertainty, we run 463 pseudo-experiments according the probability distribution of our observable. We find a significance of 55 for the hypothesis $\mathfrak{m}_{12}[C] > 1$ already with the 463 events from run2 at the LHC.

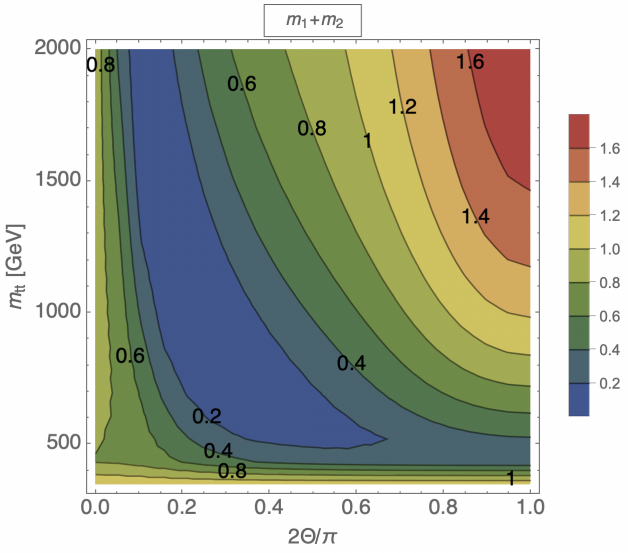


FIG. 3. The observable $\mathfrak{m}_{12}[C]$ as a function of the kinematical variables Θ and $m_{t\bar{t}}$ across the entire available space.

	(run 2) $\mathcal{L} = 140$ fb^{-1}	(Hi-Lumi) $\mathcal{L} = 3$ ab^{-1}
events	463	9727

TABLE I. Number of expected events in the kinematical region $m_{tt} > 900$ GeV and $0.85 < x < 1$.

A segmentation of the kinematical window into smaller bins (the values of which can then be collected in a χ^2 test) improves the significance of the violation, as shown in [12].

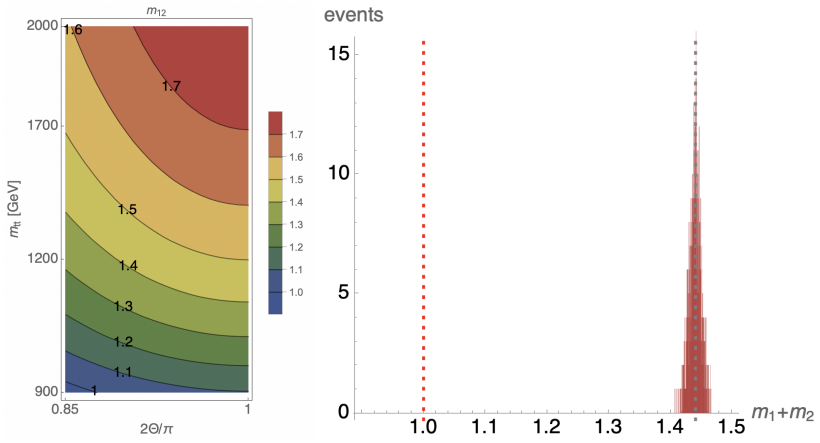


FIG. 4. On the left: The observable $\mathfrak{m}_{12}[C]$ in the kinematical window $m_{t\bar{t}} > 900$ GeV and $2\Theta/\pi > 0.85$. On the right: The statistical distribution for 463 events (with mean value 1.44 and dispersion $\sigma = 0.008$) compared with the critical value 1 above which Bell inequalities are violated.

The main source of theoretical uncertainty comes from higher order QCD corrections to the LO values of the C_{ij} matrix elements in Eq. (35). Following the results in [28, 38], where the NLO QCD corrections have been computed, we find that the error induced by these missing corrections to the largest eigenvalues in Eq. (36) is of the order of 8%, which gives approximatively a 10% uncertainty on the main entanglement observables in the relevant kinematic

regions. Small sources of theoretical uncertainties come from the PDF and the top-quark mass, but these are negligible. By comparing results with two different set of PDF, we estimate the related uncertainty to be of the order of per mille. This is of the same order as the uncertainty induced by top-quark mass, obtained by varying its mass within the two standard deviation of its experimental value.

Concerning other sources of uncertainties, we stress here that the analysis is not affected by possible backgrounds. In the top-quark pair production, the background consists of extra contributions to the $\ell^-\ell^+\nu\bar{\nu}b\bar{b}$ final state, which are negligible once the kinematic of the two on-shell top quarks is fully reconstructed. Further sources of background include $t\bar{t}W$ or $t\bar{t}Z$ as well as di-boson events, and misidentification of leptons—which amount to a few percent of the total. Another source of background is provided by the Z+jets events, whose numbers, after the cuts, is comparable to the other backgrounds aforementioned.

It goes without saying that this is an estimate that does not take into account the systematic errors inherent in the procedure of obtaining the observable from the actual data. Taking the result in [12] as guidance, we must be ready to see the significance drop by about one order of magnitude.

D. New physics: the magnetic dipole moment

As a benchmark in searching for new physics, we consider the presence of a magnetic dipole operator in the coupling between the top quark and the gluons:

$$\mathcal{L}_{\rm dipole} = -\mu\,\frac{g_s}{2m_t}\,\bar{t}\,\sigma^{\mu\nu}\,T^a\,t\,G^a_{\mu\nu}\,. \tag{37}$$

In comparing our results with those following the conventions of the SMEFT, with the magnetic dipole Lagrangian for the top quark expressed in a $SU(2)_L$ invariant way as

$$\mathcal{L}'_{\rm dipole} = \frac{c_{tG}}{\Lambda^2}\big(\mathcal{O}_{tG}+\mathcal{O}^\dagger_{tG}\big) \quad \text{with} \quad \mathcal{O}_{tG} = g_s\left(\bar{Q}_L\,\sigma^{\mu\nu}\,T^a\,t_R\right)\tilde{H}G^a_{\mu\nu}\,, \tag{38}$$

one finds

$$\mu = -\frac{\sqrt{2}m_t v}{\Lambda^2}c_{tG}\ , \tag{39}$$

which implies that $c_{tG}/\Lambda^2 = 0.1/[1\text{TeV}]^2$ corresponds to $\mu = -0.006$. Notice the change of sign. Above, Q_L and t_R stands for the $SU(2)_L$ left-handed doublet of top-bottom quarks and right-handed top quark fields respectively, while $\tilde{H}$ is as usual the dual of the $SU(2)_L$ doublet Higgs field, with SM vacuum expectation value v given by $\langle 0|\tilde{H}|0\rangle = (v/\sqrt{2},0)$.

The addition of an effective magnetic dipole moment term to the SM Lagrangian, gives rise in general to further mixture contributions, thus counteracting the generation of entanglement of the $t\bar{t}$ spin state produced by the SM interaction. Specifically, using the same notations introduced in Section III.A and the coefficients collected in the Appendix, in the $q\bar{q}$ production channel, again for transversally produced top quark pair ($\Theta = \pi/2$), the two-spin density matrix can still be expressed as the convex combination in (28), but with the parameter λ replaced by

$$\tilde{\lambda} = \frac{\beta_t^2}{2-\beta_t^2+9\mu f_{q\bar{q}}} \simeq \lambda - \mu\frac{9f_{q\bar{q}}\beta_t^2}{(2-\beta_t^2)^2}\ , \quad \text{with} \quad f_{q\bar{q}} = \frac{N_c^2-1}{N_c^2}\ . \tag{40}$$

At threshold, $\rho^{(q\bar{q})}_{t\bar{t}}$ is still the totally mixed, unentangled state $\rho^{(1)}_{\rm mix}$ as before, but at high momentum, $\rho^{(q\bar{q})}_{t\bar{t}}$ is no longer maximally entangled as $\tilde{\lambda} = 1 - 9\,\mu f_{q\bar{q}} < 1$. Notice that the convexity condition $\tilde{\lambda}\in[0,1]$ requires $\mu \geq 0$.

The case of the gg production channel is more involved. Nevertheless, at threshold the presence of the magnetic dipole moment contribution is ineffective and $\rho^{(gg)}_{t\bar{t}} = \rho^{(-)}$, still maximally entangled. On the other hand, for non-vanishing β_t, the spin density matrix can be expressed, at least for $\beta_t \geq 1/\sqrt{2}$, as the following mixture of four contributions:

$$\rho^{(gg)}_{t\bar{t}} = \tilde{a}\rho^{(+)} + \tilde{b}\rho^{(-)} + \tilde{c}\rho^{(1)}_{\rm mix} + \tilde{d}\rho^{(3)}_{\rm mix}\ , \tag{41}$$

where

$$\tilde{a} = \frac{F_{gg}}{\tilde{A}}\beta_t^2\big(2\beta_t^2-1\big)\ , \quad \tilde{b} = \frac{F_{gg}+7\mu f_{gg}}{\tilde{A}}(1-\beta_t^2)\ , \quad \tilde{c} = \frac{4F_{gg}}{\tilde{A}}\beta_t^2(1-\beta_t^2)\ , \quad \tilde{d} = \frac{7\mu f_{gg}}{\tilde{A}}\beta_t^2\ , \tag{42}$$

with

$$\tilde{A} = F_{gg}\left(1 + 2\beta_t^2 - 2\beta_t^4\right) + 7\mu f_{gg} \ , \quad \text{with} \quad F_{gg} = \frac{N_c^2 - 2}{64 N_c} \quad \text{and} \quad f_{gg} = \frac{1}{N_c(N_c^2 - 1)} \ . \tag{43}$$

As $\beta_t \to 1$, $\rho_{t\bar{t}}^{(gg)}$ remains a mixture of the density matrices $\rho^{(+)}$ and $\rho_{\rm mix}^{(3)}$, with mixing parameter $\tilde{a} = 1 - \tilde{d} = F_{gg}/(F_{gg} + 7\mu f_{gg})$, and thus with entanglement content no longer maximal. It is precisely the loss of entanglement induced by the presence of a non-vanishing magnetic dipole moment contribution both in the $q\bar{q}$ and gg production channels that allows the bound on the magnitude of the extra, effective parameter μ, to be obtained.

As $\mathcal{L}_{\rm dipole}$ is here treated as a small perturbation to the SM Lagrangian, only the lowest order contributions in μ are retained in the evaluation of the top-pair spin state $\rho_{t\bar{t}}$ and in the entries of the corresponding correlation matrix $C_{ij} = {\rm Tr}[\rho_{t\bar{t}}\,(\sigma_i \otimes \sigma_j)]$. As a consequence, the condition of positivity of the matrix $\rho_{t\bar{t}}$ might not be automatically guaranteed, and therefore it needs to be imposed in order to get physically tenable results: this might lead to possible constraint on the range of the values that the parameter μ can take.

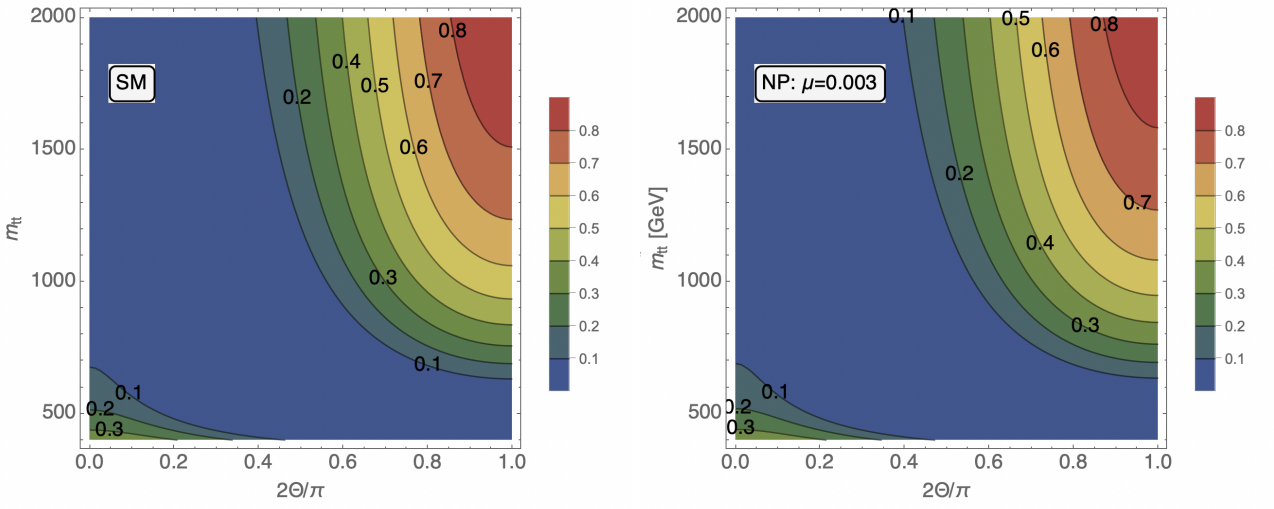


FIG. 5. On the left: Concurrence $\mathcal{C}[\rho]$ in the SM as a function of the kinematical variables Θ and $m_{t\bar{t}}$. On the right: Concurrence with new physics (NP): magnetic dipole moment with $\mu = 0.003$.

The comparison between SM and new physics entanglement is best done by means of the concurrence observable $\mathcal{C}[\rho]$. As before, the presence of only one off-diagonal matrix element in the matrix C, as given in Eq. (35), makes possible to write the concurrence in a simple analytic form as

$$\mathcal{C}[\rho] = \frac{1}{2}\max\left[0,\, |C_{rr} + C_{kk}| - (1 - C_{nn}),\, \sqrt{(C_{rr} - C_{kk})^2 + 4C_{rk}^2} - |1 - C_{nn}|\right] \tag{44}$$

Fig. 5 shows the concurrence in the whole kinematical region for the SM and in the presence of the magnetic dipole operator for the value of $\mu = 0.003$. In both cases, the entanglement grows as we reach into larger energies and larger scattering angles.

Fig. 6 shows the kinematical region $m_{t\bar{t}} > 900$ GeV and $2\Theta/\pi > 0.85$ where the relative difference Δ between SM and new physics (with $\mu = 0.003$) is largest and equal to about 3%. This result is in agreement with what found in [20] (with $c_{tG} = -0.1$ for $\Lambda = 1\,\text{TeV}$). We concentrate on this kinematical window to define the corresponding distribution of the values of the concurrence. The distribution for the SM has a central value 0.705, that in presence of the new physics becomes 0.693.

As in the case of the operator $\mathfrak{m}_{12}[C]$, a segmentation of the window into smaller bins improves the separation between SM and new physics and can be implemented to further strengthen the bound.

By running the toy Monte Carlo described in Section II for the distributions corresponding to SM and new physics, we find that, with the 463 events of LHC run2, a separation of 2.4σ is possible down to the value of $\mu = 0.003$.

This result must be compared with current determinations [39, 40] based on single observables which find a weaker bound around $\mu = 0.02$. It is comparable to that obtained from the EFT global fit [41] which utilize multiple observables. We expect that when the new quantum probe of entanglement is added to the other data of the EFT global fit, it will improve the overall sensitivity.

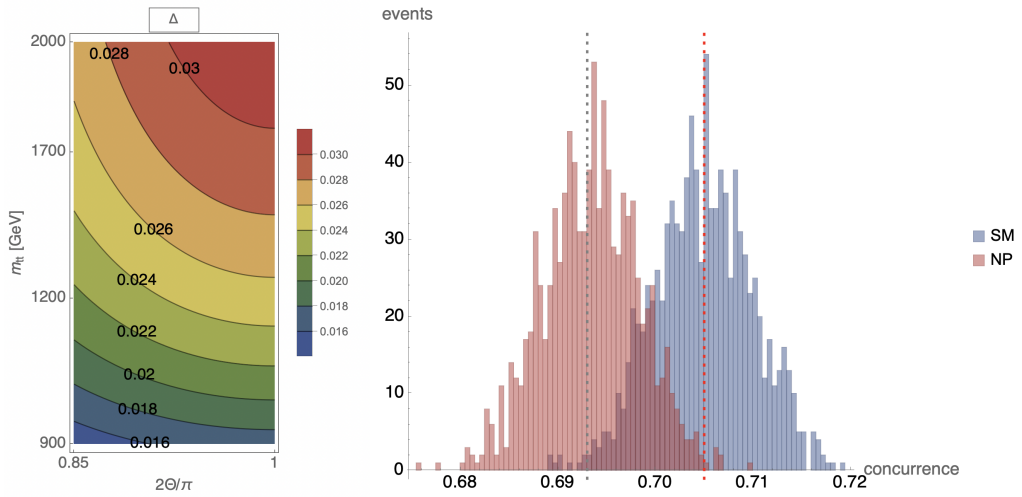


FIG. 6. On the left: Percent difference in concurrence $\mathcal{C}[\rho]$ between SM and new physics ($\mu = 0.003$) in the kinematical window $m_{t\bar{t}} > 900$ GeV and $2\Theta/\pi > 0.85$ where Δ is defined as the difference between SM and new physics over the mean value of the SM. On the right: The statistical distributions around the central values 0.705 and 0.693 for the SM and the new physics, respectively.

1. *Consistency of the approximations*

The estimates we have performed are based on three approximations which must be verified for consistency.

First of all, the linear approximation in the inclusion of the new physics is justified as long as the dipole operator, which scales with the energy of the process, is much smaller than the SM contribution. A rough estimate is provided by taking $m_{t\bar{t}} \simeq 1000$ GeV (the upper bound of our kinematical region) and $\mu \simeq 0.003$ (the benchmark value of the dipole). We have that the new physics term is order

$$\frac{m_{t\bar{t}}\,\mu}{2m_t} \simeq 0.01 \tag{45}$$

smaller than the SM and therefore the linear approximation of retaining only single insertions of the dipole operator seems to be justified.

Since the chromo-magnetic operator is an effective operators of dimension 5, its effect grows with the energy. The relevance of inserting twice this operator with respect to the single insertion becomes relevant only in kinematic regions of top-pair invariant masses that are close to the breaking of the perturbative expansion of the effective theory. We have restricted our analysis to effective scales below such a region. In particular, in the plot of Fig. 5, the limit $\mu = 0.003$ corresponds to an effective scale associated to the chromo-magnetic operator of order 100 TeV, which is much above the maximum range considered $m_{t\bar{t}} \sim 2$ TeV. Then, for invariant masses $m_{t\bar{t}} < O(1\text{ TeV})$, the quadratic contributions of the magnetic-dipole operator is expected to be negligible because proportional to terms of the order of $O(m^2_{t\bar{t}}/\Lambda^2)$. Accordingly, quadratic corrections are expected to be very small. This is confirmed by the analysis in [20] at the LO which shows that the effect of terms quadratic in the dipole operator is negligible in the kinematical region we have considered. A NLO computation appeared recently in [42].

Secondly, the same estimate in Eq. (45) also shows that the SMEFT operator expansion is justified even with an operator like the magnetic dipole that grows with the CM energy. At least for CM energies up to and around 1 TeV the correction is perturbative.

Finally, a source of concern comes about the size of QCD NLO terms with respect to the new physics term. The one-loop QCD corrections give rise to a dipole operator with coefficient

$$-\frac{\alpha_s}{\pi}\frac{m_t^2}{m_{t\bar{t}}^2}\log\frac{m_{t\bar{t}}^2}{m_t^2} \tag{46}$$

which, in the relevant kinematical window, is about 4 times smaller than the NP term with $\mu = 0.003$. Therefore, the QCD contribution to the dipole operator can be neglected, as we did, but a full QCD NLO estimate, though computationally challenging, will be necessary if the limit is to be strengthened.

E. The semi-leptonic decays of the top quark

The above analysis is done on the pseudo-observables defined in terms of the top-quark pairs. In the final analysis, these must be computed in terms of actual observables, namely the momenta of the final leptons coming from the decay of the top quarks. Introducing the angles

$$\cos\theta_+^a = \hat{\ell}_+ \cdot \hat{a} \quad \text{and} \quad \cos\theta_-^b = \hat{\ell}_- \cdot \hat{b}\,, \tag{47}$$

where $\hat{b} = -\hat{a}$ and $\hat{a} \in \{\hat{k},\ \hat{r},\ \hat{n}\}$, the cross section is given by

$$\frac{1}{\sigma}\frac{\mathrm{d}\sigma}{\mathrm{d}\Omega_+\mathrm{d}\Omega_-} = \frac{1}{16\pi^2}\Big(1 + B_- \cdot \hat{\ell}_+ + B_+ \cdot \hat{\ell}_- - \hat{\ell}_- \cdot C \cdot \hat{\ell}_+\Big) \tag{48}$$

so that, in the absence of acceptance cuts, the elements of the matrix C can be expressed [31] as

$$C_{ab}\big[m_{t\bar{t}}, \cos\Theta\big] = -9\ \frac{1}{\sigma}\int d\xi_{ab}\frac{d\sigma}{d\xi_{ab}}\xi_{ab}\,, \tag{49}$$

where we defined

$$\xi_{ab} = \cos\theta_+^a \cos\theta_-^b\,, \tag{50}$$

and with the residual dependence of the cross section σ on intrinsic kinematic variables made explicit in the argument of the matrix elements.

Such analysis based on the actual data can only be done by the experimental collaborations. It requires the full simulation of the detector, an estimate of systematic errors and the reconstruction efficiency. We are aware that a significant deterioration in significance will take place.

IV. RESULTS: TAU LEPTON PAIRS

The case in which the states produced by the interaction are τ leptons can be discussed along the same lines as for the top quarks. The dominant process is the Drell-Yan production in which the quarks go either into a photon or a Z-boson which, in turn, decay into the τ-lepton pair. In addition to the production, in this case we also have the process in which the τ leptons originate from the Higgs boson decay. We discuss the possible role of quantum entanglement in both these two physics processes.

A. Drell-Yan

The production of τ-lepton pairs via Drell-Yan in the SM receives contributions from the s-channel photon, the Z-boson and their interference. They provide an ideal laboratory for studying entanglement. Because the fewer the contributions, the larger the entanglement (as mixing diminishes quantum correlations), we expect this to be larger at low-energies (where the photon diagram dominates) or around the Z-boson pole (where the Z-boson diagram dominates). At low energies, the cross section is dominated by the photon term which produces entangled τ-lepton pairs, while at high-energies all terms contribute and entanglement is suppressed. Around the Z-boson pole the cross section is dominated by the corresponding term with maximal entanglement.

B. Entanglement in $\tau\bar{\tau}$ production

As in the case of the top-quark pair production, the two spin-1/2 state is described by a density matrix of the general form (1), whose entries depend on the kinematic variable $\beta_\tau = \sqrt{1 - 4m_\tau^2/m_{\tau\bar{\tau}}^2}$, with $m_{\tau\bar{\tau}}$ the τ-pair invariant mass, and on the scattering angle Θ.

Using the same reference frame and notation introduced as for the top pair production in Section III.A, and again focusing on the situation of transversally produced lepton pairs ($\Theta = \pi/2$), as previously mentioned, one can distinguish three kinematical regions: The first, at low energies, $m_{\tau\bar{\tau}} \ll m_Z$, where photon exchange is dominating, the intermediate one, $m_{\tau\bar{\tau}} \simeq m_Z$, dominated by the Z exchange and finally the high energy one, $m_{\tau\bar{\tau}} \gg m_Z$.

With the help of the results collected in the Appendix, in the low-energy regime (for which $m_{\tau\bar{\tau}} \ll m_Z$) and for all quark production channels, the τ-pair spin state can be represented by the convex combination as in (28),

$$\rho_{\tau\bar{\tau}} = \lambda\rho^{(+)} + (1-\lambda)\rho^{(1)}_{\rm mix} \quad \text{with} \quad \lambda = \frac{\beta_\tau^2}{2-\beta_\tau^2} \in [0,1]\,; \tag{51}$$

at threshold, $\beta_\tau \simeq 0$, the state is a totally mixed one, with no quantum correlations, while as $\beta_\tau \to 1$, the spins of the τ-lepton pair tend to be generated in a maximally entangled state.

As the Z-channel starts to become relevant, this entanglement is however progressively lost due to the mixing between the photon and Z contribution. Nevertheless, a revival of entanglement occurs as the Z channel become dominant, $m_{\tau\bar{\tau}} \simeq m_Z$; in this region, with the notation and conventions introduced in the Appendix, the two-spin density matrix can be described by the following convex combination, for all quark production channels :

$$\rho_{\tau\bar{\tau}} = \lambda\tilde{\rho}^{(+)} + (1-\lambda)\tilde{\rho}^{(2)}_{\rm mix}\,, \qquad \lambda = \frac{(g_A^\tau)^2 - (g_V^\tau)^2}{(g_A^\tau)^2 + (g_V^\tau)^2}\,, \tag{52}$$

where,

$$\tilde{\rho}^{(2)}_{\rm mix} = \frac{1}{2}\Big(|{\rm RR}\rangle\langle{\rm RR}| + |{\rm LL}\rangle\langle{\rm LL}|\Big)\,, \tag{53}$$

while,

$$\tilde{\rho}^{(+)} = |\tilde{\psi}^{(+)}\rangle\langle\tilde{\psi}^{(+)}|\,, \qquad |\tilde{\psi}^{(+)}\rangle = \frac{1}{\sqrt{2}}\Big(|{+}{-}\rangle + |{-}{+}\rangle\Big)\,, \tag{54}$$

is a projector on a Bell state as in (24), but now expressed in terms of the eigenvectors of σ_x. It turns out that $\lambda \simeq 1$, so that $\rho_{\tau\bar{\tau}}$ is very close to the maximally entangled state $\tilde{\rho}^{(+)}$.

Finally, in the high energy regime ($m_{\tau\bar{\tau}} \gg m_Z$) both photon and Z channel contribute, and their mixing lead to a rapid depletion of entanglement. Indeed, for each $q\bar{q}$ production channel, the τ-pair spin correlations can be described in terms of the following density matrix:

$$\rho_{\tau\bar{\tau}} = \lambda^q\rho^{(+)} + (1-\lambda^q)\tilde{\rho}^{(2)}_{\rm mix}\,, \qquad \lambda^q = \frac{1-R^q_-}{1+R^q_+}\,, \tag{55}$$

where $\rho^{(+)}$ is as in (24), while

$$R^q_\pm = \frac{\chi^2(m^2_{\tau\bar{\tau}})\big[(g^q_A)+(g^q_V)\big]\big[(g^\tau_A)\pm(g^\tau_V)\big]}{(Q^q)^2(Q^\tau)^2 + 2\,{\rm Re}\chi(m^2_{\tau\bar{\tau}})\,Q^qQ^\tau\,g^q_Vg^\tau_V}\,. \tag{56}$$

Specifically, in the case of the u quark production channel, one finds $\lambda^u \simeq 0.7$, so that some entanglement is preserved, while for the d quark production channel, as $\lambda^d \simeq 0.1$, entanglement is essentially lost.

For completeness, it should be noticed that each τ lepton is produced in a partially polarized state, as some of the single-spin polarization coefficient $B_i^\pm$ in (1) are non-vanishing (see Appendix). This is particularly relevant for the quark d production channel, where the magnitude of these single particle terms is of the same order of the entries of the correlation matrix C_{ij}, while for the u production channel they are about one order of magnitude smaller. This implies that the full density matrix describing the τ-pair spin state $\rho_{\tau\bar{\tau}}$ is really in this case a mixture of (55) with additional states further reducing in general its entanglement content.

In addition, as discussed below, the full correlation matrix C_{ij} is obtained by putting together all relevant $q\bar{q}$-production channel contributions, weighted by suitable luminosity functions and with appropriate normalization: this leads to further mixing and in general to additional loss of entanglement.

C. Computing the observables

As before, we compute all the entries of the correlation matrix C_{ij} from the process

$$p + p \to \tau^- + \tau^+\,. \tag{57}$$

with the unpolarized cross section given by

$$\frac{{\rm d}\sigma}{{\rm d}\Omega\,{\rm d}m_{\tau\bar{\tau}}} = \frac{\alpha^2\beta_\tau}{64\pi^2 m^2_{\tau\bar{\tau}}}\Big\{L^{uu}(\tau)\,\tilde{A}^{uu}[m_{\tau\bar{\tau}},\Theta] + \big[L^{dd}(\tau)+L^{ss}(\tau)\big]\,\tilde{A}^{dd}[m_{\tau\bar{\tau}},\Theta]\Big\} \tag{58}$$

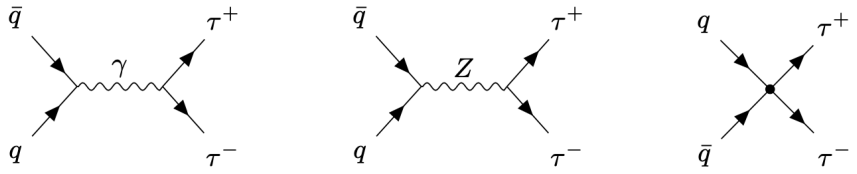


FIG. 7. Feynman diagrams for $\tau^-\tau^+$ production. On the right, the contact interaction (see Eq. (61)).

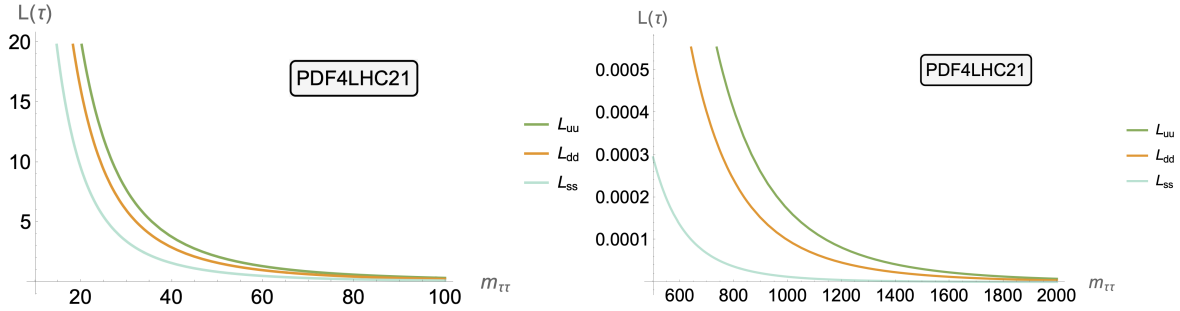


FIG. 8. Parton luminosity functions: The up quark luminosity is about 28% larger than the down quark luminosity at threshold, then increasing to about 38% around the Z-boson pole and eventually reaching 70% around 1 TeV.

with $L^{qq}(\tau)$ the parton luminosity functions of section II, $\tau = m_{\tau^-\tau^+}/\sqrt{s}$ and $\alpha = e^2/4\pi$. The explicit expressions for $\tilde{A}^{uu,dd}(m_{\tau\bar{\tau}})$ are given in the Appendix.

We combine the two channels (see Fig. 7) $u + \bar{u} \to \tau^- + \tau^+$ (which enters with factors function of $Q_u = 2/3$) and $d + \bar{d} \to \tau^-\tau^+$ and $s + \bar{s} \to \tau^-\tau^+$ (which enters with factors function of $Q_d = -1/3$) by weighting the respective contributions through the parton luminosity functions

$$L^{qq}(\tau) = \frac{4\tau}{\sqrt{s}} \int_\tau^{1/\tau} \frac{\mathrm{d}z}{z} q_q(\tau z) q_{\bar{q}}\left(\frac{\tau}{z}\right) \tag{59}$$

where the $q(x)$ are the PDFs for respectively the u, d and s quarks. As before, their numerical values are those provided by PDF4LHC21 [35] for $\sqrt{s} = 13$ TeV and factorization scale $q_0 = m_{\tau\bar{\tau}}$ (see Fig. 8).

Therefore, we have that

$$C_{ij}[m_{t\bar{t}}, \Theta] = \frac{L^{uu}(\tau)\, \tilde{C}^{uu}_{ij}[m_{\tau\bar{\tau}}, \Theta] + \left[L^{dd}(\tau) + L^{ss}(\tau)\right] \tilde{C}^{dd}_{ij}[m_{\tau\bar{\tau}}, \Theta]}{L^{uu}(\tau)\, \tilde{A}^{uu}[m_{\tau\bar{\tau}}, \Theta] + \left[L^{dd}(\tau) + L^{ss}(\tau)\right] \tilde{A}^{dd}[m_{\tau\bar{\tau}}, \Theta]}\,, \tag{60}$$

where the down-quark luminosities can be grouped together because they multiply the same correlation functions. The expression in Eq. (60) must be expanded in the case of new physics by retaining the linear terms.

D. Bell inequalities

The values of the observable $\mathfrak{m}_{12}[C]$ are shown in Fig. 9 across the entire kinematical space. The figure confirms the qualitative analysis of section IV.B. It shows that, for large scattering angles, entanglement is close to maximal (that is,$\mathfrak{m}_{12}[C]$ close to 2) where the invariant mass of the τ-lepton pairs selects one of the two possible channels with either the photon or the Z-boson exchange dominating.

We take the kinematical window where $20 < m_{\tau\bar{\tau}} < 45$ and $2\Theta/\pi > 0.80$ as the most favorable to test the Bell inequalities and there estimate the operator $\mathfrak{m}_{12}[C]$. In this window the mean value of $\mathfrak{m}_{12}[C]$ is 1.88. The number of expected events at the LHC is large (see Table II in which the cross sections are computed by running MADGRAPH5 [36] at the LO and then correcting by the κ-factor given at the NNLO [43]) and we show the statistical significance of the hypothesis $\mathfrak{m}_{12}[C] > 1$ (as obtained by running the toy Monte Carlo described in section II) for

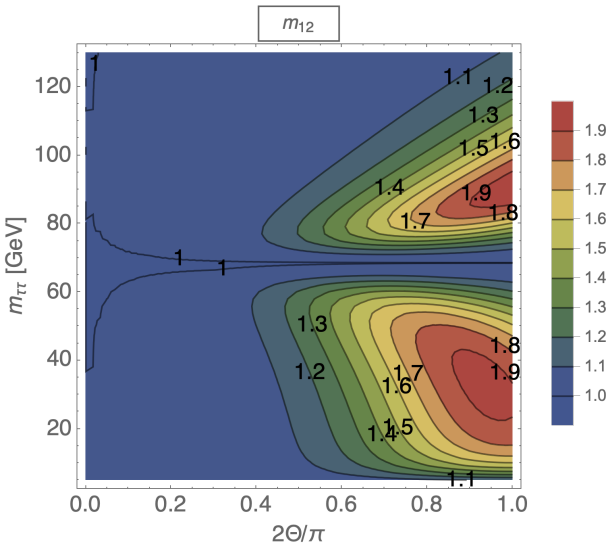


FIG. 9. Eigenvalues $\mathfrak{m}_{12}[C]$ as a function of the kinematical variables Θ and $m_{t\bar{t}}$ across the entire available space.

	(run 2) $\mathcal{L} = 140$ fb^{-1}	(Hi-Lumi) $\mathcal{L} = 3$ ab^{-1}
events	1.1×10^6	2.2×10^7

TABLE II. Number of expected events in the kinematical region $20 < m_{\tau\bar{\tau}} < 45$ GeV and $2\Theta/\pi > 0.80$

the case of having just 100 events (Fig. 10). The statistical significance is huge: more than 100. Indeed, this seems to be the process where the experimental confirmation of the violation of Bell inequalities is most likely thanks to the large number of events available (as opposed to the scarcity of events with the required energy in the case of the top quark).

The main source of theoretical uncertainty on the entanglement observables of the τ lepton pairs comes from the choice of the PDF, which is negligible in the relevant kinematic regions and giving an effect of the order of a per mille. As it was for the case of the top-quark pairs, here too the possible backgrounds are negligible once the tagging on the exclusive decays modes of the τ and the kinematic cuts to reconstruct its on-shell mass are employed.

E. New physics: Contact interactions

The simplest new physics that can enter the Drell-Yan process is a contact interaction among quarks and τ-leptons. Such a contact interaction mediates a process in which the quarks directly produce the leptons (see Fig 7).

The most general contact operators for the production of τ-leptons from quarks can be written, in chiral components, as

$$\mathcal{L}_{cc} = -\frac{4\pi}{\Lambda^2}\eta_{LL}(\bar{q}_L\gamma^\alpha q_L)\,(\bar{\tau}_L\gamma_\alpha\tau_L) - \frac{4\pi}{\Lambda^2}\eta_{RR}(\bar{q}_R\gamma^\alpha q_R)\,(\bar{\tau}_R\gamma_\alpha\tau_R) - \frac{4\pi}{\Lambda^2}\eta_{LR}(\bar{q}_L\gamma^\alpha q_L)\,(\bar{\tau}_R\gamma_\alpha\tau_R) - \frac{4\pi}{\Lambda^2}\eta_{RL}(\bar{q}_R\gamma^\alpha q_R)\,(\bar{\tau}_L\gamma_\alpha\tau_L)\,. \quad (61)$$

These contact operators can be thought, in a UV complete theory, as arising from the exchange of a scalar lepto-quark. The scale Λ in Eq. (61) could be of the same order of the mass scale of the corresponding new physics particles. The exchange of a vector lepto-quark leads to contact operators with no interference terms with the SM diagrams, in the quark and lepton massless limit, and therefore less constrained. The scale Λ controls the size of these new-physics terms; the factor 4π is conventional and is there to remind us that the UV physics could come from a strong-coupling regime.

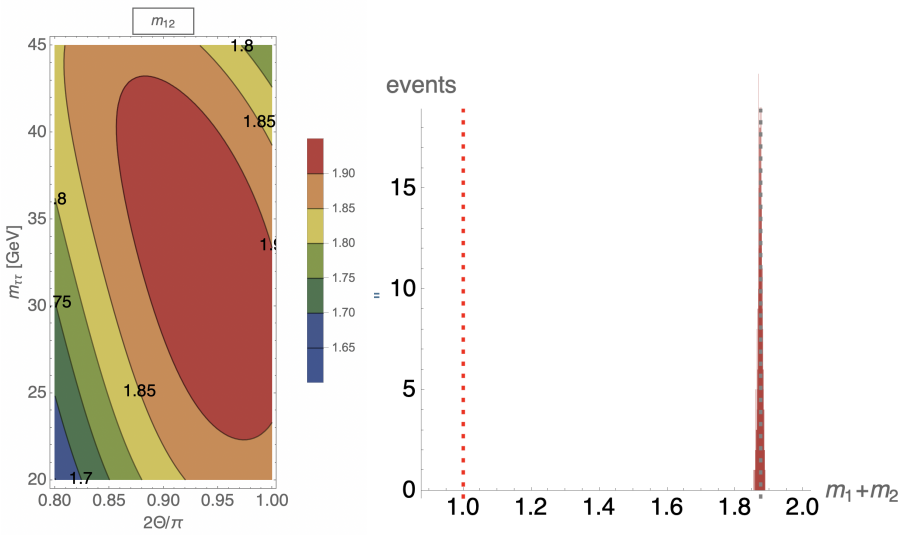


FIG. 10. On the left: The kinematical window ($20 < m_{\tau\bar{\tau}} < 45$, $2\Theta/\pi > 0.80$) where the Bell inequality is to be tested. On the right: The statistical distribution for 100 events around the mean value 1.88 with dispersion given by $\sigma = 0.006$.

To gauge the effect of these terms is sufficient to take one of them. The function $\tilde{A}$ and $\tilde{C}_{ij}$ for the operator LR (the third term in Eq. (61)) are given in Appendix with $\eta_{LR} = 1$.

Based on general grounds, all operators in Eq. (61) give the same order of magnitude effect. Indeed, in model independent analysis, it is customary to assume the contributions from different operators to be uncorrelated, due to different potential NP contributions to each of the corresponding Wilson coefficients. Therefore, the bounds obtained from each separate contribution to the entanglement, are expected to be the same order of the other operators, which only differs for a different chirality structure.

The addition of such an effective contact interaction term to the SM Lagrangian modifies the picture we drew about the entanglement of the τ-lepton pairs in Section IV.B For a given quark $q\bar{q}$ production channel and in the high energy regime ($m_{\tau\bar{\tau}} \gg m_Z$), the τ-pair spin correlations can again be described in terms of the convex combination in (55), but with the parameter λ^q replaced by

$$\tilde{\lambda}^q = \lambda^q \left[1 + \eta \left(\frac{\tilde{R}^q_-}{1 + R^q_+} - \frac{\tilde{R}^q_+}{1 - R^q_-} \right) \right] , \quad \tilde{R}^q_\pm = \frac{Q^q Q^\tau \pm \chi(m^2_{\tau\bar{\tau}}) \left[(g^q_A) + (g^q_V) \right] \left[(g^\tau_A) \pm (g^\tau_V) \right]}{(Q^q)^2 (Q^\tau)^2 + 2\,\mathrm{Re}\chi(m^2_{\tau\bar{\tau}})\, Q^q Q^\tau\, g^q_V g^\tau_V} . \tag{62}$$

where $\eta = m^2_{\tau\bar{\tau}}/\alpha\Lambda^2$. For the u-quark production channel $\tilde{\lambda}^u \simeq \lambda^u(1+\eta/4)$, while for the d-quark production channel one finds $\tilde{\lambda}^d \simeq \lambda^d(1-3\eta)$. As both λ^u and λ^d are less than 1 and η is small, one can get both an increase and a decrease of the τ-pair spin correlations according to the sign of η, without violating the requirement of the positivity of the density matrix $\rho_{\tau\bar{\tau}}$. It is precisely this change in the entanglement content of the τ-pair spin state induced by the presence of the contact term contribution, both in the $u\bar{u}$ and $d\bar{d}$ production channels, that makes possible obtaining bounds on the magnitude of the new physics scale Λ.

	(run 2) $\mathcal{L} = 140$ fb^{-1}	(Hi-Lumi) $\mathcal{L} = 3$ ab^{-1}
events	27	573

TABLE III. Number of expected events in the kinematical region $m_{\tau^+\tau^-} > 800$ GeV and $0.85 < x < 1$.

As we already discussed, the entanglement becomes larger in the kinematical regions where either the photon or the Z-boson diagram dominates. Because the new physics terms increase as the energy in the CM, these regions—being as they are at relatively low-energies—are not favorable for distinguishing between SM and new physics. It is at higher energies, just below 1 TeV that the two can best be compared. At these energies, the amount of entanglement

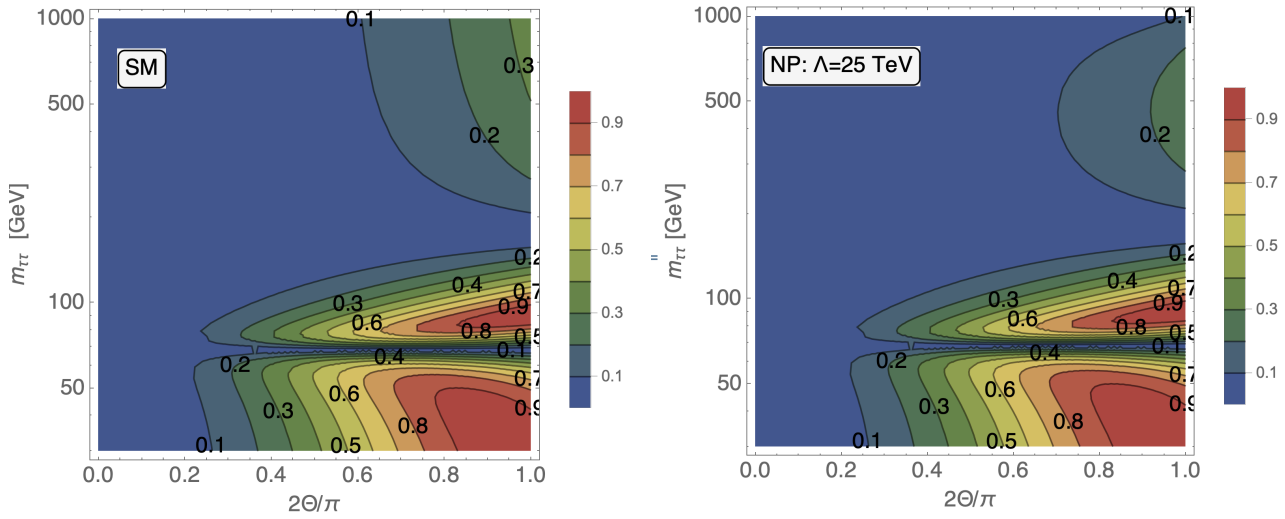


FIG. 11. On the left: Concurrence $\mathcal{C}[\rho]$ in the SM as a function of the kinematical variables Θ and $m_{t\bar{t}}$. On the right: Concurrence with new physics (NP) (with $\Lambda = 25$ TeV). The invariant squared mass is on a logarithmic scale in both figures.

is modest but very sensitive to the addition of new terms in the amplitude. We therefore consider the kinematical region $m_{\tau\bar{\tau}} > 800$ as a compromise between having enough events and having new-physics effects sizable.

As previously mentioned, a new feature of the τ-lepton case is the non-vanishing of some single polarization $B_i^{\pm}$ terms in the spin density matrix (1), which were instead all zero in in the case of the top-quark pairs spin states. Their presence makes the extraction of the concurrence $\mathcal{C}[\rho]$ possible only numerically.

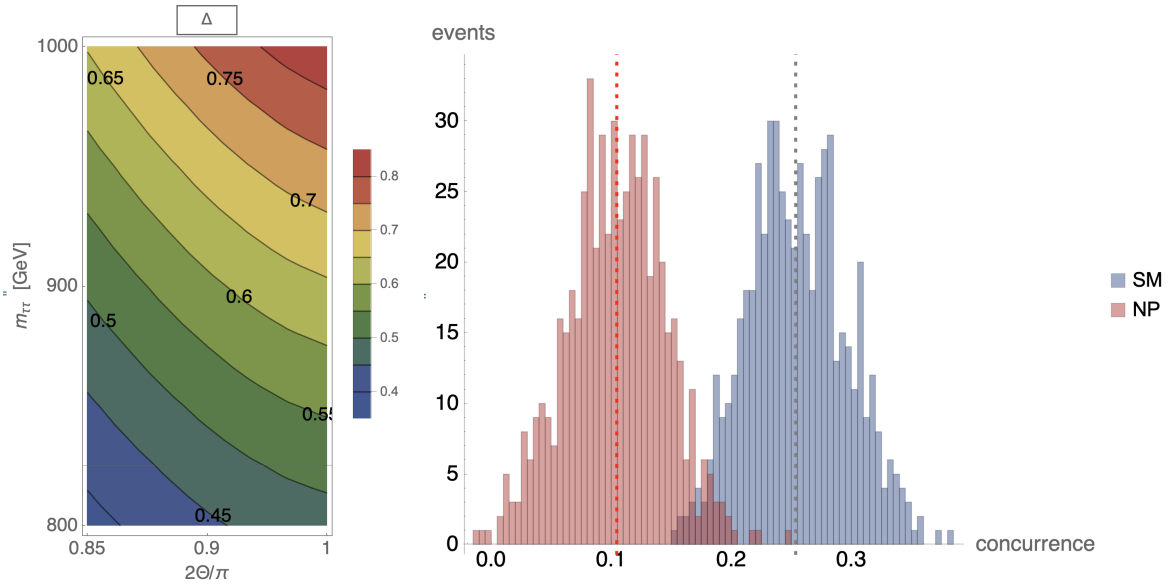


FIG. 12. On the left: Percent difference in concurrence $\mathcal{C}[\rho]$ in the kinematical window $0.85 < 2\Theta/\pi < 1$ and $800 < m_{t\bar{t}} < 1000$ between the SM and new physics (with $\Lambda = 25$ TeV or, equivalently, $c = 0.02$) where Δ is defined as the difference between SM and new physics over the mean value for the SM. On the right: Statistical distributions for the 573 events expected at Hi-Lumi for the SM (blue bins, mean value 0.25) and the new physics (red bins, mean value 0.10).

The left side of Fig. 12 shows the kinematical region $m_{\tau\bar{\tau}} > 800$ GeV and $0.85 < x < 1$ where the relative difference Δ between SM and new physics (with $\Lambda = 25$ TeV) is largest and equal to about 70%. The mean value of $\mathcal{C}[\rho]$ for the SM is 0.25, 0.10 for the new physics, the dispersion is about $\sigma = 0.04$. Such a large effect shows that the contact interaction and its scrambling of the two τ-lepton polarizations is a very effective way of changing the concurrence of

their spins.

The number of events at high-energy is shown in Table III. They turn out to be too few at LHC run2. The right side of Fig. 12 shows how new physics can be distinguished from SM with a significance of 3.7 for a contact interaction with a scale $\Lambda = 25$ TeV with 573 events (Hi-Lumi). This result compares favorably with current determinations of four-fermion operators [44, 45] (see also, the review in [46]).

The value $\Lambda = 25$ TeV corresponds to $c = 0.02$ for $\Lambda = 1\,\text{TeV}$ in the SMEFT notation where the contact operator we are considering is given by

$$\frac{c}{\Lambda^2}(\bar{q}_L\gamma^\alpha q_L)\,(\bar{\tau}_R\gamma_\alpha\tau_R)\,. \tag{63}$$

This value is such as to make the estimate in a region where both the SMEFT expansion is safe and the NLO contributions smaller. Contrary to the magnetic dipole momentum in the top-quark case, in the τ-lepton case EW and QCD NLO corrections are expected to be much smaller than the effect of the contact interaction terms.

F. The τ-lepton decays

The τ lepton decays as

$$\begin{aligned}\tau^- &\to A + \nu_\tau \\ &\not\mapsto A = e^-\bar{\nu}_e,\, \mu^-\bar{\nu}_\mu,\, \pi^-,\, \rho^-,\, a_1 \ldots\end{aligned} \tag{64}$$

with

$$\text{BR}\,(\ell^-\bar{\nu}_\ell\nu_\tau) \simeq 35\%, \quad \text{BR}\,(\pi^-\nu_\tau) \simeq 11\%, \quad \text{and} \quad \text{BR}\,(\rho^-/a_1\nu_\tau) \simeq 26\%\,. \tag{65}$$

These decays taken together account for more than 80% of all decays.

The angular distribution of the decay products can be used to determine the polarization of the τ lepton. The decay mode $\tau^- \to \pi^-\nu_\tau$ has a distribution

$$\frac{1}{\Gamma}\frac{\mathrm{d}\Gamma}{\mathrm{d}z} = \frac{1}{2}(1 + P_\tau z)\,, \tag{66}$$

where $z = \cos\theta$—the angle being defined with respect to the charged final state. Eq. (66) is the same as in the case of the top-quarks and the same procedure to compute the coefficients C_{ij} can be used here. Unfortunately the branching ratio for the two τs to simultaneously decay in this channel is small and around 1%. Yet the large number of expected events around $m_{\tau\bar{\tau}} \simeq 30$ GeV makes the analysis of the Bell inequalities violation possible.

The leptonic decay mode $\tau^- \to \ell^-\bar{\nu}_\ell\nu_\tau$ has a distribution

$$\frac{1}{\Gamma}\frac{\mathrm{d}\Gamma}{\mathrm{d}z} = \frac{1}{2}(1-z)\Big[(5 + 5z - 4z^2) + P_\tau(1 + z - 8z^2)\Big]\,, \tag{67}$$

which has only a weak dependence on the polarization [47].

Therefore one has to resort to the two decays $\tau \to \rho\nu_\tau$ and $\tau \to a_1\nu_\tau$. The reconstruction of the coefficients C_{ij} for these channels depends on that of the polarizations of the mesons [47]. For this reason, the analysis can only be done by means of a full simulation. The relevance of the physics of entanglement we discussed might encourage the on-going efforts in this direction by the experimental collaborations. The effect is there—waiting to be extracted from the data.

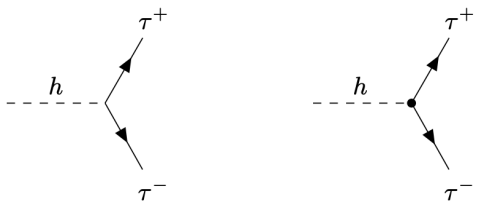


FIG. 13. Feynman diagrams for $\tau^-\tau^+$ production. On the right, a possible CP odd vertex.

G. Higgs boson decay

The decay of the Higgs boson into a pair of fermions (see, Fig. 13) or—as we discuss in the next section, two photons—provides a physical process very similar to those utilized in atomic physics for studying entanglement. Because the final states originate from a scalar state, their entanglement is obvious as much as the correlation between their angular momenta.

1. *Bell inequalities*

The interaction Lagrangian for the decay of the Higgs boson into a pair of τ leptons is given by

$$\mathcal{L}_{\rm SM} = \frac{m_\tau}{v}\bar{\tau}\tau\, h\,, \tag{68}$$

where v is the vacuum expectation value of the Higgs field h. On the basis of this interaction term, the elements of the matrix C_{ij} entering the tau lepton-pair spin density matrix (1) can be easily computed and given by

$$C = \begin{pmatrix} 1 & 0 & 0 \\ 0 & 1 & 0 \\ 0 & 0 & -1 \end{pmatrix}\,, \tag{69}$$

where the C matrix above is defined on the $\{\hat{n}, \hat{r}, \hat{k}\}$ spin basis as in Eq. (35). The sum of the square of the two largest eigenvalues gives $\mathfrak{m}_{12}[C] = 2$, so that the Bell inequality (5) is maximally violated.

	(run 2) $\mathcal{L} = 140$ fb^{-1}	(Hi-Lumi) $\mathcal{L} = 3$ ab^{-1}
events	2.3×10^5	5.1×10^6

TABLE IV. Number of expected events in the Higgs boson decay into $\tau^+\tau^-$ pairs.

Since there is no kinematical dependence, we simply give the uncertainty as $1/\sqrt{N}$ with N the number of events. Given the maximal violation of Bell inequalities and the large number of events (see Table IV in which the cross sections are computed by running MADGRAPH5 [36] at the LO and then correcting by the κ-factor given at the N3LO+N3LL [48]), the significance can be huge. As shown in Fig 14 in the case of 1000 events, the significance of the hypothesis $\mathfrak{m}_{12}[C] > 1$ is 10. Unfortunately in this kinematical region the tail of the pole of the Z-boson still dominates and gives a background that has to be reduced in order to proceed with the physical analysis.

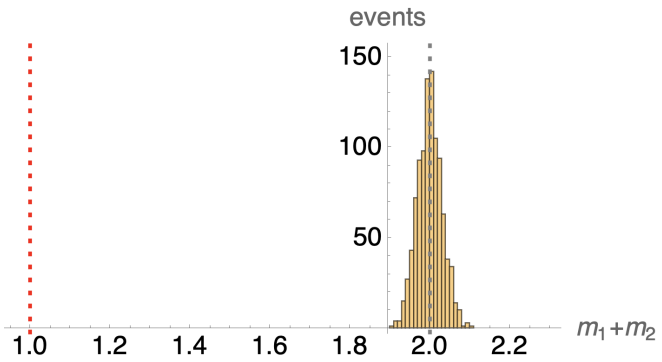


FIG. 14. Significance of the violation of Bell inequality in the decay of the Higgs boson in τ^--τ^+ and photon pairs (as discussed below). Given the large number of events, the Gaussian distribution around the value 2 is very peaked ($\sigma = 1/\sqrt{N}$) and the statistical significance large. As an example, we draw the case $N = 1000$ for which the statistical significance of $\mathfrak{m}_{12}[C] > 1$ is 32.

2. Constraints on new physics

We would like to study the entanglement of the two τ leptons in the presence of new physics. The Higgs boson in the SM is a scalar CP even state. A CP odd component can be introduced by a vertex as that in the Lagrangian [49–51]

$$\mathcal{L}_{\text{CP odd}} = i\frac{m_\tau}{v}\bar{\tau}\gamma_5\tau\, h\,. \tag{70}$$

For a recent review on possible CP odd interactions of the Higgs boson, see [53].

Combining the two interactions, mimicking for instance the two doublet Higgs models, we have

$$\cos\varphi\,\mathcal{L}_{\text{SM}} + \sin\varphi\,\mathcal{L}_{\text{CP odd}}\,, \tag{71}$$

where the parameter φ modulates the amount of new physics.

Taking the two vertices in Eq. (71) together should provide the means to constrain the new-physics CP odd vertex. Absorptive contributions are for the moment excluded, so that the coupling constants are assumed to be real.

Notice that, concerning the specific case of the on-shell Higgs decay in two fermions, the new physics parametrization given in Eq. (71) is also the most general one. Indeed, in the case of both the Higgs and fermions fields on-shell, the potential contribution of Lorentz invariant operators of higher dimensions can always be projected into the coupling structure provided by the renormalizable Lagrangian in Eq. (71).

With this generalized interaction Lagrangian, the elements of the correlation matrix C in Eq. (35) become

$$C = \begin{pmatrix} \dfrac{\beta_\tau^2\cos^2\varphi - \sin^2\varphi}{\beta_\tau^2\cos^2\varphi + \sin^2\varphi} & -\dfrac{\beta_\tau \sin 2\varphi}{\beta_\tau^2\cos^2\varphi + \sin^2\varphi} & 0 \\ \dfrac{\beta_\tau \sin 2\varphi}{\beta_\tau^2\cos^2\varphi + \sin^2\varphi} & \dfrac{\beta_\tau^2\cos^2\varphi - \sin^2\varphi}{\beta_\tau^2\cos^2\varphi + \sin^2\varphi} & 0 \\ 0 & 0 & -1 \end{pmatrix}, \tag{72}$$

where now $\beta_\tau = \sqrt{1-4m_\tau^2/m_h^2}$. This result has already been found in [49, 52]. Then, the eigenvalues of the $M = C^T C$ matrix are equal to $(1,1,1)$ and the operator $\mathfrak{m}_{12}[C] = 2$, showing a maximal violation of the Bell inequalities.

Similarly, the resulting concurrence is still maximal,

$$\mathcal{C}[\rho] = 1 \tag{73}$$

as it is independent from φ. This surprising result can be understood as follows. At tree level, the interaction in (71) produce pair of leptons that turn out to be totally unpolarized, but highly correlated in spin. In fact, choosing the z-axis along the τ^- direction of flight in the Higgs rest frame, and neglecting terms of order $(m_\tau/m_h)^2$, so that $\beta_\tau \simeq 1$, the spin state of the τ-lepton pair turns out to be [50]:

$$|\psi_{\tau\bar{\tau}}\rangle = \frac{1}{\sqrt{2}}\Big(|01\rangle + e^{2i\varphi}\,|10\rangle\Big)\,, \tag{74}$$

where $|0\rangle$ and $|1\rangle$ are as before the eigenvectors of σ_z, representing the projection of the lepton spins along the z axis. As the CP transformation reverses these spin projections, the pure state (74) is a $CP = 1$ state for $\varphi = 0$, the usual SM result, while it is a $CP = -1$ state for $\varphi = \pi/2$. In addition, it is maximally entangled for all values of φ: indeed, the trace over either leptons of the corresponding density matrix gives a totally unpolarized state: $\text{Tr}_{1,2}\big[|\psi_{\tau\bar{\tau}}\rangle\langle\psi_{\tau\bar{\tau}}|\big] = \mathbb{1}/2$. As a consequence, in this particular case, the entanglement content of the lepton pair spin state can not be used to bound CP-odd additions to the SM as the spin quantum correlations are insensible to the angle φ.

A difference in entanglement shows in the concurrence only in the presence of an absorptive term—it makes the entanglement no longer unaffected by the CP odd term. This result is reminiscence of what happens in the Kaon system where we need both a CP-violating and a CP-conserving phase in order to be able to see direct CP-violation.

Such an absorptive part can come in the SM from QED loop correction to the vertex as the two final leptons exchange a photon but is very small. A phase could also be produced by the new physics term but we do not explore it further since is model dependent and it unavoidably introduces extra parameters and an uncertainty that is hard to judge.

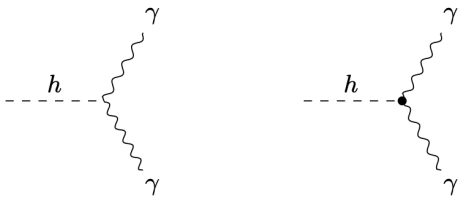


FIG. 15. Feynman diagrams for the Higgs boson h into two photons. The dot stands for the CP-odd vertex.

V. RESULTS: TWO PHOTONS

The entanglement of a system of two photon has been discussed in [54]. Here we examine it as the final states of the decay of the Higgs boson. In more than one way, this system is even closer than the Higgs boson decay into τ-lepton pairs discussed in the previous section to what is done in atomic physics, where the polarizations of photons originating in atomic transitions are discussed.

A. Bell inequalities

The Higgs boson h decays into two photons via an effective coupling $g_{\gamma\gamma h}$ provided in the SM by loop contributions. The Lagrangian is given by

$$\mathcal{L} = -\frac{1}{4}\, g_{\gamma\gamma h}\, h\, F^{\mu\nu} F_{\mu\nu}\,, \tag{75}$$

where $F^{\mu\nu}$ is the field strength of the photon.

The corresponding polarized amplitude square is

$$|\mathcal{M}_h|^2 = |g_{\gamma\gamma h}|^2 V^{\mu\nu}(k_1,k_2) V^{\rho\sigma}(k_1,k_2) \left[\varepsilon_\mu^{\lambda_1}(k_1)\varepsilon_\rho^{\lambda_1'*}(k_1)\right]\left[\varepsilon_\nu^{\lambda_2}(k_2)\varepsilon_\sigma^{\lambda_2'*}(k_2)\right]\,, \tag{76}$$

where $V^{\mu\nu}(k_1,k_2) = g^{\mu\nu}(k_1\cdot k_2) - k_1^\nu k_2^\mu$. Notice that, gauge invariance is guaranteed by the Ward Identities $k_1^\mu V_{\mu\nu}(k_1,k_2) = k_2^\nu V_{\mu\nu}(k_1,k_2) = 0$.

The projection on the linear polarizations can be performed by substituting the terms in square brackets with the corresponding density matrix $\rho_{\mu\nu}$ given in Eq. (22), and using the method explained in Section II. After summing over all photons polarizations, we obtain the unpolarized amplitude square

$$|\bar{\mathcal{M}}_h|^2 = |g_{h\gamma\gamma}|^2 m_h^4/2\,, \tag{77}$$

to which corresponds the width $\Gamma = g_{h\gamma\gamma}^2 m_h^3/(64\pi^2)$.

After normalization over the unpolarized square amplitude in Eq. (81), we find that the correlation matrix C is

$$C = \begin{pmatrix} 1 & 0 & 0 \\ 0 & -1 & 0 \\ 0 & 0 & 1 \end{pmatrix}\,. \tag{78}$$

in the basis of the Stokes parameters $\{\xi_1,\xi_2,\xi_3\}$ for the linear polarizations as defined in Eq. (22). For the matrix C in Eq. (78), the operator $\mathfrak{m}_{12}[C] = 2$ and the Bell inequalities are maximally violated.

	(run 2) $\mathcal{L} = 140$ fb^{-1}	(Hi-Lumi) $\mathcal{L} = 3$ ab^{-1}
events	8854	1.8×10^5

TABLE V. Number of expected events in the Higgs boson decay into two photons.

To estimate the uncertainty, we consider a Gaussian distribution around the value 2. The number of events expected in the production and decay of the Higgs boson into two photons is shown in Table V in which the cross sections are estimated at the LO by means of MADGRAPH5 [36] and then corrected by the κ-factor as estimated at the N3LO+N3LL [48]. Given the large number of events, this distribution has a rather sharp peak. The statistical significance of the violation is shown in Fig. 14 (Section 4.7) for 1000 events, the same way we did for the case of the Higgs boson decaying into a pair of τ-leptons. Already for this number of events the violation is statistically significant. This a test well worth doing but it requires the detection of the polarization of the two photons.

B. New physics

As discussed in the case of the decay into τ-leptons, the Higgs boson could have a CP odd vertex from a new physics contribution. In the case of two final photons, it would decay just like the neutral pion π^0 decays into two photons via the anomaly. Then, it is useful to parametrize the corresponding effective Lagrangian as

$$\mathcal{L}' = -\frac{1}{4}\,\tilde{g}_{h\gamma\gamma}\,h\,F^{\mu\nu}\tilde{F}_{\mu\nu}\,, \tag{79}$$

where $\tilde{F}_{\mu\nu} = 1/2\epsilon_{\mu\nu\alpha\beta}F^{\alpha\beta}$ is the dual field strength of the photon, with $\epsilon_{\mu\nu\alpha\beta}$ the Levi-Civita antisymmetric tensor satisfying $\epsilon_{0123} = 1$. Then, the corresponding polarized square amplitude is given by

$$|\mathcal{M}'_h|^2 = |\tilde{g}_{\gamma\gamma h}|^2\tilde{V}^{\mu\nu}(k_1,k_2)\tilde{V}^{\rho\sigma}(k_1,k_2)\left[\varepsilon_\mu^{\lambda_1}(k_1)\varepsilon_\rho^{\lambda'_1\,*}(k_1)\right]\left[\varepsilon_\nu^{\lambda_2}(k_2)\varepsilon_\sigma^{\lambda'_2\,*}(k_2)\right]\,, \tag{80}$$

where $\tilde{V}_{\mu\nu}(k_1,k_2) = \epsilon_{\mu\nu\alpha\beta}k_1^\alpha k_2^\beta$. Notice that, gauge invariance of the amplitude is automatically guaranteed by the antisymmetric properties of $\epsilon_{\mu\nu\alpha\beta}$. For the unpolarized amplitude square, we obtain

$$|\bar{\mathcal{M}}_h|^2 = |\tilde{g}_{h\gamma\gamma}|^2 m_h^4/2\,. \tag{81}$$

If we now combine the two Lagrangians as

$$\mathcal{L}^{\rm total} = \frac{g_{\gamma\gamma h}}{4}\left[\left(h\,F^{\mu\nu}F_{\mu\nu}\right) + z\left(h\,F^{\mu\nu}\tilde{F}_{\mu\nu}\right)\right] \tag{82}$$

by collecting the respective coefficients in the parameter $z \equiv \tilde{g}_{\gamma\gamma h}/g_{\gamma\gamma h}$, we might expect to be able to study the effect of the new physics on the entanglement of the two final photons.

A non-vanishing interference among the two contributions arises in the polarized contributions to the square amplitude generated by the Lagrangian in Eq. (82), while it vanishes in the unpolarized case.

From the Lagrangian in Eq. (82) we obtain the correlation matrix (in the Stokes parameter basis)

$$C = \begin{pmatrix} \dfrac{1-z^2}{1+z^2} & 0 & \dfrac{2\,z}{1+z^2} \\ 0 & -1 & 0 \\ -\dfrac{2\,z}{1+z^2} & 0 & \dfrac{1-z^2}{1+z^2} \end{pmatrix}. \tag{83}$$

Non-vanishing contributions to the B_i coefficients arise due to the interference term; they are given by

$$B_2^+ = -B_2^- = i\frac{2|z|}{1+|z|^2}\,,\; B_1^\pm = B_3^\pm = 0. \tag{84}$$

They represents the polarization of the single photons. The B_i coefficients are purely imaginary and cancel out in the matrix R (see Eq. (3) in Section II) which gives us the concurrence.

As in the case of the final two τ leptons, for real coefficients in the Lagrangians in Eq. (82), our expectation of extracting bounds on the new physics is frustrated and the overall entanglement is not affected and

$$\mathcal{C}[\rho] = 1\,. \tag{85}$$

even in the presence of new physics.

The presence of an absorptive part in one or both the two couplings $g_{\gamma\gamma h}$ and $\tilde{g}_{\gamma\gamma h}$, by inducing a phase $\delta = \arg z$, would make the concurrence sensitive to the new physics. In this case, the matrix C would become

$$C = \begin{pmatrix} \dfrac{1-|z|^2}{1+|z|^2} & 0 & \dfrac{2|z|\cos\delta}{1+|z|^2} \\ 0 & -1 & 0 \\ -\dfrac{2|z|\cos\delta}{1+|z|^2} & 0 & \dfrac{1-|z|^2}{1+|z|^2} \end{pmatrix}, \tag{86}$$

and (for z and δ small) the concurrence is given by

$$\mathcal{C}[\rho] = 1 - |z|\,\delta\,, \tag{87}$$

thus probing the presence of the CP-odd term.

A phase is present in the SM vertex and comes mainly from the absorptive part of the b-quark loop in the effective coupling between the Higgs boson and the two photons. In particular, assuming the $\tilde{g}_{\gamma\gamma h}$ real, for the phase δ in the SM framework we get $\delta \sim -4 \times 10^{-4}$. Even if included, this contribution is too small to make a difference.

One may speculate about the presence of a phase in the CP odd vertex. Since the size of it depends on the specific model and the uncertainty would be hard to gauge, we do not to pursue this possibility further.

C. Detecting photon polarizations

The possibility of measuring photon polarizations depends on their energy. For high-energy photons, the dominant process is pair production as the photons fly through matter. There are two possible processes: the electron interacting with the nuclei (A) or the atom electrons:

$$\begin{aligned} \gamma + A &\to A + e^+ + e^- \\ \gamma + e^- &\to e^- + e^+ + e^-\,, \end{aligned} \tag{88}$$

with the latter dominating in the energy range we are interested in.

For a polarized photon, the Bethe-Heitler cross section for the *Bremsstrahlung* production of electron pairs depends also on the azimuthal angles $\varphi_\pm$ of the produced electron and positron [55, 56] as

$$\frac{\mathrm{d}s}{\mathrm{d}\varphi_+ \mathrm{d}\varphi_-} = \sigma_0 \Big[X_{\rm un} + X_{\rm pol}\, P_\gamma \cos(\varphi_+ - \varphi_-) \Big]\,, \tag{89}$$

where P_γ is the linear polarization fraction of the incident photon, $X_{\rm un}$ and $X_{\rm pol}$ are the unpolarized and polarized coefficients respectively, which depend on the kinematical variables. The explicit form of the cross section in Eq. (89) can be found in [57]. The relevant azimuthal information comes from the dependence of the cross section on the a-coplanarity of the outgoing electron and positron. The measure of the relative angle between these momenta gives information on the polarization of the photon.

Even though this possibility is not currently implemented at the LHC, detectors able to perform such a measurement are under discussion for astrophysical γ rays [58] and an event generator to simulate the process already exists [59] and has been implemented within GEANT [60] (for a recent review, see [61]).

VI. SUMMARY AND OUTLOOK

Our exploration of the use of quantum entanglement at colliders shows that it can provide new tests of quantum mechanics as well as a very promising new tool in the study of the SM as well as its possible extensions leading to new physics.

The best system by far where to test the violation of Bell inequalities is the decay of the Higgs boson. The decay of the Higgs boson into a pair of τ-leptons seems already feasible with the data of run2 at the LHC although one has to disentangle this channel from the tail of the Z-boson pole that still dominates at values of the invariant mass around the Higgs boson mass. The decay of the Higgs boson into two photons, while equally promising, requires a dedicated detector in order to measure the photon polarizations. A similar test is also possible in the production of

top-quark and τ-lepton pairs, with the latter the most promising within the kinematical windows just above threshold and around the Z-boson pole.

Searching for constraints to new physics is possible by means of the entanglement between the spins of pairs of particles produced in the collisions. We find the concurrence $\mathcal{C}[\rho]$ an observable very sensitive to any physics beyond the SM. The use of this tool is illustrated by considering a magnetic dipole operator in the case of having top-quark pairs and a contact interaction for the case of τ leptons. Because the impact of the higher order operators corresponding to this new physics grows with the energy of the process, they must be tested at the highest energy available. In this regime, the top-quark pairs are mostly entangled while the τ leptons less so. Nevertheless, what counts is the relative change in entanglement and both cases show a promising power in constraining the size of the new physics better than current limits based on total cross sections or classical correlations.

Our analysis is about pseudo-observables at the level of the parton production processes and decays. The last word—comprising a full analysis of all uncertainties, statistical as well as systematic—can only come from the extraction of the entanglement observables $\mathfrak{m}_{12}[C]$ and $\mathcal{C}[\rho]$ from the data (or at least from a full simulation of them). Though this is a challenging problem—which can only be properly addressed by the experimental collaborations—it is well worth the effort because of the improved sensitivity to which the new tools give access.

ACKNOWLEDGMENTS

MF thanks M. Casarsa for help on the implementation of the toy Monte Carlo and L. Marzola for help on the PDFs. We thank M. Kadastik, L. Marzola, J. Pata and C. Veelken for discussions on the physics of the τ leptons. We thank M. Casarsa and F. Longo for discussions on the detection of photon polarizations.

Appendix A: Cross section functions

In this Appendix we provide the explicit expression for the functions $\tilde{A}$, $\tilde{C}_{ij}$ and $\tilde{B}_i$ in the cross section of the processes discussed in the main text. The tilde above these quantities reminds us that they have to be normalized, like in Eq. (34) and Eq. (60), dividing by the unpolarized cross section to give the entries of Eq. (1).

1. Top-quark pairs

a. *Standard Model*

Below, we write the $\tilde{A}^{q\bar{q}}$, $\tilde{B}_i^{qq}$, and $\tilde{C}_{ij}^{qq}$ coefficients for the $t\bar{t}$ pair production via $q\bar{q}$ and gg scattering in the SM framework. These functions were calculated in [62, 63]; we report them for ease of reading:

$$\tilde{A}^{gg} = F_{gg}\Big[1 + 2\beta_t^2 \sin^2\Theta - \beta_t^4\left(1 + \sin^4\Theta\right)\Big], \tag{A1a}$$

$$\tilde{C}_{nn}^{gg} = -F_{gg}\Big[1 - 2\beta_t^2 + \beta_t^4\left(1 + \sin^4\Theta\right)\Big], \tag{A1b}$$

$$\tilde{C}_{rr}^{gg} = -F_{gg}\Big[1 - \beta_t^2\left(2 - \beta_t^2\right)\left(1 + \sin^4\Theta\right)\Big], \tag{A1c}$$

$$\tilde{C}_{kk}^{gg} = -F_{gg}\Big[1 - \beta_t^2\frac{\sin^2 2\Theta}{2} - \beta_t^4\left(1 + \sin^4\Theta\right)\Big], \tag{A1d}$$

$$\tilde{C}_{kr}^{gg} = \tilde{C}_{rk}^{gg} = F_{gg}\,\beta_t^2\sqrt{1-\beta_t^2}\sin 2\Theta\sin^2\Theta \tag{A1e}$$

$$\tilde{B}_k^{gg} = \tilde{B}_r^{gg} = \tilde{B}_n^{gg} = 0\,, \tag{A1f}$$

with $F_{gg} = \dfrac{N_c^2\left(1+\beta_t^2\cos^2\Theta\right)-2}{64N_c\left(1-\beta_t^2\cos^2\Theta\right)^2}$ and

$$\tilde{A}^{q\bar{q}} = F_{q\bar{q}}\Big(2-\beta_t^2\sin^2\Theta\Big), \tag{A2a}$$
$$\tilde{C}_{nn}^{q\bar{q}} = -F_{q\bar{q}}\,\beta_t^2\sin^2\Theta, \tag{A2b}$$
$$\tilde{C}_{rr}^{q\bar{q}} = F_{q\bar{q}}\Big(2-\beta_t^2\Big)\sin^2\Theta, \tag{A2c}$$
$$\tilde{C}_{kk}^{q\bar{q}} = F_{q\bar{q}}\Big(2\cos^2\Theta+\beta_t^2\sin^2\Theta\Big), \tag{A2d}$$
$$\tilde{C}_{kr}^{q\bar{q}} = \tilde{C}_{rk}^{q\bar{q}} = F_{q\bar{q}}\sqrt{1-\beta_t^2}\sin 2\Theta, \tag{A2e}$$
$$\tilde{B}_k^{gg} = \tilde{B}_r^{gg} = \tilde{B}_n^{gg} = 0\,, \tag{A2f}$$

with $F_{q\bar{q}} = \dfrac{1}{2N_c^2}$.

b. *New physics: magnetic moment dipole*

Here, we collect the results for the coefficients $\tilde{A}^{q\bar{q}}$, $\tilde{B}_i^{qq}$, and $\tilde{C}_{ij}^{qq}$ for the magnetic moment dipole in Eq. (37) in which we retained only the interference with the corresponding SM amplitudes. They were computed in [31]:

$$\tilde{A}^{gg} = f_{gg}^{(1)}\left[N_c^2\left(1+\beta_t^2\cos^2\Theta\right)-2\right]\mu, \tag{A3a}$$
$$\tilde{C}_{nn}^{gg} = f_{gg}^{(1)}\left(2-N_c^2\right)\mu, \tag{A3b}$$
$$\tilde{C}_{rr}^{gg} = f_{gg}^{(2)}\left[N_c^2\left(-1+\beta_t^4\cos^2\Theta\sin^4\Theta\right)+(N_c^2-2)\beta_t^2\big(\sin^2\Theta+\cos^4\Theta\big)+2\right]\mu, \tag{A3c}$$
$$\begin{aligned}\tilde{C}_{kk}^{gg} = f_{gg}^{(2)}\,\frac{1}{1-\beta_t^2}\Bigg\{&N_c^2\Big[-1-\beta_t^2\big(-2+\cos^4\Theta\big)+\beta_t^6\cos^2\Theta\big(-1-\cos^2\Theta+\cos^4\Theta\big)\\&-\beta_t^4\big(\sin^2\Theta-2\cos^4\Theta+\cos^6\Theta\big)\Big]\\&+2\Big[1+\beta_t^4\big(1+\cos^2\Theta-\cos^4\Theta\big)+\beta_t^2\big(-2-\cos^2\Theta+\cos^4\Theta\big)\Big]\Bigg\}\mu,\end{aligned} \tag{A3d}$$
$$\begin{aligned}\tilde{C}_{kr}^{gg} = \tilde{C}_{rk}^{gg} = f_{gg}^{(2)}\,\frac{\beta_t^2\sin 2\Theta}{2\sqrt{1-\beta_t^2}}\Bigg\{&\frac{N_c^2}{2}\Big[-2\cos^2\Theta-\beta_t^4\cos^2\Theta\sin^2\Theta+\beta_t^2\big(1+3\cos^2\Theta-2\cos^4\Theta\big)\Big]\\&-1+\big(2-\beta_t^2\big)\cos^2\Theta\Bigg\}\mu\,,\end{aligned} \tag{A3e}$$
$$\tilde{B}_k^{gg} = \tilde{B}_r^{gg} = \tilde{B}_n^{gg} = 0\,, \tag{A3f}$$

and

$$\tilde{A}^{q\bar{q}} = \frac{f_{q\bar{q}}}{2}\,\mu, \tag{A4a}$$
$$\tilde{C}_{nn}^{q\bar{q}} = 0, \tag{A4b}$$
$$\tilde{C}_{rr}^{q\bar{q}} = \frac{f_{q\bar{q}}}{2}\left(1-\cos^2\Theta\right)\,\mu, \tag{A4c}$$
$$\tilde{C}_{kk}^{q\bar{q}} = \frac{f_{q\bar{q}}}{2}\,\cos^2\Theta\,\mu, \tag{A4d}$$
$$\tilde{C}_{kr}^{q\bar{q}} = \tilde{C}_{rk}^{q\bar{q}} = f_{q\bar{q}}\,\frac{\big(2-\beta_t^2\big)\sin 2\Theta}{8\sqrt{1-\beta_t^2}}\,\mu, \tag{A4e}$$
$$\tilde{B}_k^{q\bar{q}} = \tilde{B}_r^{q\bar{q}} = \tilde{B}_n^{q\bar{q}} = 0\,, \tag{A4f}$$

with $f_{gg}^{(1)} = \dfrac{1}{N_c(N_c^2-1)}\dfrac{1}{(1-\beta_t^2\cos^2\Theta)}$, $f_{gg}^{(2)} = \dfrac{1}{N_c(N_c^2-1)}\dfrac{1}{(1-\beta_t^2\cos^2\Theta)^2}$ and $f_{q\bar{q}} = \dfrac{N_c^2-1}{N_c^2}$.

2. τ-lepton pairs

a. *Standard Model*

Below, we write the $\tilde{A}^{q\bar{q}}$, $\tilde{B}_i^{qq}$, and $\tilde{C}_{ij}^{qq}$ coefficients for the $\tau^+\tau^-$ pair production via $q\bar{q}$ scattering in the SM framework:

$$\tilde{A}^{q\bar{q}} = F_{q\bar{q}}\Big\{ Q_q^2 Q_\tau^2 \Big[2-\beta_\tau^2\sin^2\Theta\Big] + 2Q_qQ_\tau \mathrm{Re}\big[\chi(m_{\tau\bar{\tau}}^2)\big]\,\Big[2\beta_\tau g_A^q g_A^\tau\cos\Theta + g_V^q g_V^\tau\left(2-\beta_\tau^2\sin^2\Theta\right)\Big] + \big|\chi(m_{\tau\bar{\tau}}^2)\big|^2\,\Big[\left(g_V^{q2}+g_A^{q2}\right)\left(2g_V^{\tau 2}+2\beta_\tau^2 g_A^{\tau 2}-\beta_\tau^2\left(g_V^{\tau 2}+g_A^{\tau 2}\right)\sin^2\Theta\right) + 8\beta_\tau g_V^q g_V^\tau g_A^q g_A^\tau\cos\Theta\Big]\Big\}, \tag{A5a}$$

$$\tilde{C}_{nn}^{q\bar{q}} = -F_{q\bar{q}}\beta_\tau^2\sin^2\Theta\Big\{ Q_q^2Q_\tau^2 + 2Q_qQ_\tau\mathrm{Re}\big[\chi(m_{\tau\bar{\tau}}^2)\big]\,g_V^q g_V^\tau - \big|\chi(m_{\tau\bar{\tau}}^2)\big|^2\left(g_V^{q2}+g_A^{q2}\right)\left(g_A^{\tau 2}-g_V^{\tau 2}\right)\Big\}, \tag{A5b}$$

$$\tilde{C}_{rr}^{q\bar{q}} = -F_{q\bar{q}}\sin^2\Theta\Big\{ \left(\beta_\tau^2-2\right)Q_q^2Q_\tau^2 + 2Q_qQ_\tau\mathrm{Re}\big[\chi(m_{\tau\bar{\tau}}^2)\big]\,g_V^q g_V^\tau\left(\beta_\tau^2-2\right) + \big|\chi(m_{\tau\bar{\tau}}^2)\big|^2\left[\beta_\tau^2\left(g_A^{\tau 2}+g_V^{\tau 2}\right)-2g_V^{\tau 2}\right]\left(g_V^{q2}+g_A^{q2}\right)\Big\}, \tag{A5c}$$

$$\tilde{C}_{kk}^{q\bar{q}} = F_{q\bar{q}}\Big\{ Q_q^2Q_\tau^2\Big[\left(\beta_\tau^2-2\right)\sin^2\Theta+2\Big] + 2Q_qQ_\tau\mathrm{Re}\big[\chi(m_{\tau\bar{\tau}}^2)\big]\,\Big[2\beta_\tau g_A^q g_A^\tau\cos\Theta + g_V^q g_V^\tau\left(\left(\beta_\tau^2-2\right)\sin^2\Theta+2\right)\Big] + \big|\chi(m_{\tau\bar{\tau}}^2)\big|^2\,\Big[8\beta_\tau g_A^q g_A^\tau g_V^q g_V^\tau\cos\Theta + \left(g_V^{q2}+g_A^{q2}\right)\left(2g_V^{\tau 2}\cos^2\Theta-\beta_\tau^2\left(g_A^{\tau 2}-g_V^{\tau 2}\right)\sin^2\Theta+2\beta_\tau^2 g_A^{\tau 2}\right)\Big]\Big\}, \tag{A5d}$$

$$\tilde{C}_{kr}^{q\bar{q}} = \tilde{C}_{rk}^{q\bar{q}} = 2F_{q\bar{q}}\sin\Theta\sqrt{1-\beta_\tau^2}\Big\{ Q_q^2Q_\tau^2\cos\Theta + Q_qQ_\tau\,\mathrm{Re}\big[\chi(m_{\tau\bar{\tau}}^2)\big]\,\Big[\beta_\tau g_A^q g_A^\tau + 2g_V^q g_V^\tau\cos\Theta\Big] + \big|\chi(m_{\tau\bar{\tau}}^2)\big|^2\,\Big[2\beta_\tau g_A^q g_A^\tau g_V^q g_V^\tau + g_V^{\tau 2}\left(g_V^{q2}+g_A^{q2}\right)\cos\Theta\Big]\Big\},$$

$$\tilde{C}_{rn}^{q\bar{q}} = \tilde{C}_{nr}^{q\bar{q}} = \tilde{C}_{kn}^{q\bar{q}} = \tilde{C}_{nk}^{q\bar{q}} = 0\,, \tag{A5e}$$

$$\tilde{B}_k^{q\bar{q}} = -2F_{q\bar{q}}\Big\{ Q_qQ_\tau\mathrm{Re}\big[\chi(m_{\tau\bar{\tau}}^2)\big]\,\Big[\beta_\tau g_A^\tau g_V^q\left(1+\cos^2\Theta\right)+2g_A^q g_V^\tau\cos\Theta\Big] + \big|\chi(m_{\tau\bar{\tau}}^2)\big|^2\,\Big[2g_A^q g_V^q\left(\beta_\tau^2 g_A^{\tau 2}+g_V^{\tau 2}\right)\cos\Theta + \beta_\tau g_A^\tau g_V^\tau\left(g_V^{q2}+g_A^{q2}\right)\left(1+\cos^2\Theta\right)\Big]\Big\}, \tag{A5f}$$

$$\tilde{B}_r^{q\bar{q}} = -2F_{q\bar{q}}\sin\Theta\sqrt{1-\beta_\tau^2}\Big\{ Q_qQ_\tau\mathrm{Re}\big[\chi(m_{\tau\bar{\tau}}^2)\big]\,\Big[\beta_\tau g_A^\tau g_V^q\cos\Theta+2g_A^q g_V^\tau\Big] + \big|\chi(m_{\tau\bar{\tau}}^2)\big|^2 g_V^\tau\Big[\beta_\tau g_A^\tau\left(g_V^{q2}+g_A^{q2}\right)\cos\Theta+2g_A^q g_V^q g_V^\tau\Big]\Big\}, \tag{A5g}$$

$$\tilde{B}_n^{q\bar{q}} = 0\,, \tag{A5h}$$

with $F_{q\bar{q}} = \dfrac{1}{16}$, $Q_{q,\tau}$ the electric charges, β_τ the $\tau^\pm$ velocity in their CM frame,

$$g_V^i = T_3^i - 2\,Q_i\sin^2\theta_W\,, \quad g_A^i = T_3^i\,, \tag{A6}$$

and

$$\mathrm{Re}\left[\chi(q^2)\right] = \frac{q^2(q^2-m_Z^2)}{\sin^2\theta_W\cos^2\theta_W\left[(q^2-m_Z^2)^2+q^4\Gamma_Z^2/m_Z^2\right]}\quad, \tag{A7}$$

$$\left|\chi(q^2)\right|^2 = \frac{q^4}{\sin^4\theta_W \cos^4\theta_W \left[(q^2 - m_Z^2)^2 + q^4\Gamma_Z^2/m_Z^2\right]}\,, \tag{A8}$$

where θ_W is the Weinberg angle, m_Z and Γ_Z the mass and total width of the Z boson respectively, and $q^2 = (q_1+q_2)^2$.

b. *New physics: Contact interactions*

Here, we write the results for the coefficients $\tilde{A}^{q\bar{q}}$, $\tilde{B}_i^{qq}$, and $\tilde{C}_{ij}^{qq}$ for the contact interaction in Eq. (61)—for the benchmark operator $\frac{4\pi}{\Lambda^2}(\bar{q}_L\gamma^\alpha q_L)\,(\bar{\tau}_R\gamma_\alpha\tau_R)$—in which we retained only the interference with the corresponding SM amplitudes:

$$\begin{aligned}\tilde{A}^{q\bar{q}} = F_\Lambda \Big\{ & Q_q Q_\tau \Big[\beta_\tau^2 \sin^2\Theta + 2\beta_\tau\cos\Theta - 2\Big] + \mathrm{Re}\big[\chi(m_{\tau\bar{\tau}}^2)\big]\,(g_V^q + g_A^q)\Big[-2g_V^\tau + 2\beta_\tau\,(g_V^\tau - g_A^\tau)\cos\Theta \\ & + \beta_\tau^2 g_A^\tau\,(1+\cos^2\Theta) + \beta_\tau^2 g_V^\tau \sin^2\Theta\Big]\Big\}\,,\end{aligned} \tag{A9a}$$

$$\tilde{C}_{nn}^{q\bar{q}} = F_\Lambda\,\beta_\tau^2\sin^2\Theta\Big\{Q_qQ_\tau + \mathrm{Re}\big[\chi(m_{\tau\bar{\tau}}^2)\big]\,\big(g_V^q+g_A^q\big)\big(g_A^\tau+g_V^\tau\big)\Big\}\,, \tag{A9b}$$

$$\tilde{C}_{rr}^{q\bar{q}} = F_\Lambda\,\sin^2\Theta\Big\{Q_qQ_\tau\,\big[\beta_\tau^2-2\big] + \mathrm{Re}\big[\chi(m_{\tau\bar{\tau}}^2)\big]\,\big(g_V^q+g_A^q\big)\Big[\beta_\tau^2\,(g_V^\tau-g_A^\tau) - 2g_V^\tau\Big]\Big\}\,, \tag{A9c}$$

$$\begin{aligned}\tilde{C}_{kk}^{q\bar{q}} = F_\Lambda\Big\{ & Q_qQ_\tau\Big[2\beta_\tau\cos\Theta - 2\cos^2\Theta - \beta_\tau^2\sin^2\Theta\Big] + \mathrm{Re}\big[\chi(m_{\tau\bar{\tau}}^2)\big]\,\big(g_V^q+g_A^q\big)\Big[-2g_V^\tau\cos^2\Theta \\ & + \beta_\tau\,(g_V^\tau-g_A^\tau)\,(2\cos\Theta-\beta_\tau) + \beta_\tau^2\,(g_A^\tau+g_V^\tau)\cos^2\Theta\Big]\Big\}\,,\end{aligned} \tag{A9d}$$

$$\begin{aligned}\tilde{C}_{kr}^{q\bar{q}} = \tilde{C}_{rk}^{q\bar{q}} = F_\Lambda\,\sqrt{1-\beta_\tau^2}\sin\Theta\Big\{ & Q_qQ_\tau\Big[\beta_\tau - 2\cos\Theta\Big] \\ & + \mathrm{Re}\big[\chi(m_{\tau\bar{\tau}}^2)\big]\,\big(g_V^q+g_A^q\big)\Big[\beta_\tau\big(g_V^\tau-g_A^\tau\big) - 2g_V^\tau\cos\Theta\Big]\Big\}\,,\end{aligned} \tag{A9e}$$

$$\tilde{C}_{rn}^{q\bar{q}} = \tilde{C}_{nr}^{q\bar{q}} = \tilde{C}_{kn}^{q\bar{q}} = \tilde{C}_{nk}^{q\bar{q}} = 0\,, \tag{A9f}$$

$$\begin{aligned}\tilde{B}_k^{q\bar{q}} = F_\Lambda\Big\{ & Q_qQ_\tau\Big[2\cos\Theta - \beta_\tau\,(1+\cos^2\Theta)\Big] + \mathrm{Re}\big[\chi(m_{\tau\bar{\tau}}^2)\big]\,\big(g_V^q+g_A^q\big)\Big[-2\beta_\tau^2 g_A^\tau\cos\Theta \\ & + \beta_\tau\big(g_A^\tau-g_V^\tau\big)\,(1+\cos^2\Theta) + 2g_V^\tau\cos\Theta\Big]\Big\}\,,\end{aligned} \tag{A9g}$$

$$\tilde{B}_r^{q\bar{q}} = F_\Lambda\,\sqrt{1-\beta_\tau^2}\sin\Theta\Big\{Q_qQ_\tau\Big[2-\beta_\tau\cos\Theta\Big] + \mathrm{Re}\big[\chi(m_{\tau\bar{\tau}}^2)\big]\,\big(g_V^q+g_A^q\big)\Big[\beta_\tau\,(g_A^\tau-g_V^\tau)\cos\Theta + 2g_V^\tau\Big]\Big\}\,, \tag{A9h}$$

$$\tilde{B}_n^{q\bar{q}} = 0\,, \tag{A9i}$$

where $F_\Lambda = \dfrac{m_{\tau\bar{\tau}}^2}{8\alpha\Lambda^2}$.

[1] R. Horodecki, P. Horodecki, M. Horodecki and K. Horodecki, "Quantum entanglement," Rev. Mod. Phys. **81**, 865-942 (2009) [arXiv:quant-ph/0702225 [quant-ph]].

[2] N. A. Tornqvist, "Suggestion for Einstein-Podolsky-Rosen Experiments Using Reactions Like $e^+e^- \to \Lambda\bar{\Lambda} \to \pi^- p\pi^+\bar{p}$," Found. Phys. **11**, 171-177 (1981).

[3] S. A. Abel, M. Dittmar and H. K. Dreiner, "Testing locality at colliders via Bell's inequality?" Phys. Lett. B **280**, 304-312 (1992)

[4] F. Benatti and R. Floreanini, *Phys. Rev. D* **57** (1998) 1332; [arXiv:hep-ph/9906272 [hep-ph]]; "Direct CP violation as a test of quantum mechanics," Eur. Phys. J. C **13**, 267-273 (2000) [arXiv:hep-ph/9912348 [hep-ph]];

R. A. Bertlmann, W. Grimus and B. C. Hiesmayr, "Bell inequality and CP violation in the neutral kaon system," Phys. Lett. A **289**, 21-26 (2001) [arXiv:quant-ph/0107022 [quant-ph]].
[5] S. Banerjee, A.K. Alok and R. MacKenzie, Eur. Phys. J. Plus **131**, 129 (2016).
[6] A. Acin, J. I. Latorre and P. Pascual, "Three party entanglement from positronium," Phys. Rev. A **63**, 042107 (2001) [arXiv:quant-ph/0007080 [quant-ph]];
J. Li and C. F. Qiao, "New Probabilities of Testing Local Realism in High Energy Physics," Phys. Lett. A **373**, 4311 (2009) [arXiv:0812.0869 [quant-ph]].
[7] S. P. Baranov, "Bell's inequality in charmonium decays $\eta_c \to \Lambda\bar{\Lambda}$, $\chi_c \to \Lambda\bar{\Lambda}$ and $J/\psi \to \Lambda\bar{\Lambda}$," J. Phys. G **35**, 075002 (2008);
S. Chen, Y. Nakaguchi and S. Komamiya, "Testing Bell's Inequality using Charmonium Decays," PTEP **2013**, no.6, 063A01 (2013) [arXiv:1302.6438 [hep-ph]];
C. Qian, J. L. Li, A. S. Khan and C. F. Qiao, "Nonlocal correlation of spin in high energy physics," Phys. Rev. D **101**, no.11, 116004 (2020) [arXiv:2002.04283 [quant-ph]].
[8] S. Banerjee, A. K. Alok, R. Srikanth and B. C. Hiesmayr, "A quantum information theoretic analysis of three flavor neutrino oscillations," Eur. Phys. J. C **75**, no.10, 487 (2015) [arXiv:1508.03480 [hep-ph]].
[9] N. Yongram and E. B. Manoukian, "Quantum field theory analysis of polarizations correlations, entanglement and Bell's inequality: explicit processes," Fortsch. Phys. **61**, 668-684 (2013) [arXiv:1309.2059 [hep-th]].
[10] A. Cervera-Lierta, J. I. Latorre, J. Rojo and L. Rottoli, "Maximal Entanglement in High Energy Physics," SciPost Phys. **3**, no.5, 036 (2017) [arXiv:1703.02989 [hep-th]]
[11] Y. Afik and J. R. M. de Nova, "Entanglement and quantum tomography with top quarks at the LHC," Eur. Phys. J. Plus **136**, no.9, 907 (2021) [arXiv:2003.02280 [quant-ph]].
[12] M. Fabbrichesi, R. Floreanini and G. Panizzo, "Testing Bell Inequalities at the LHC with Top-Quark Pairs," Phys. Rev. Lett. **127**, no.16, 16 (2021) [arXiv:2102.11883 [hep-ph]].
[13] C. Severi, C. D. Boschi, F. Maltoni and M. Sioli, "Quantum tops at the LHC: from entanglement to Bell inequalities," Eur. Phys. J. C **82**, no.4, 285 (2022) [arXiv:2110.10112 [hep-ph]].
[14] A. J. Larkoski, "General analysis for observing quantum interference at colliders," Phys. Rev. D **105**, no.9, 096012 (2022) [arXiv:2201.03159 [hep-ph]].
[15] J. A. Aguilar-Saavedra and J. A. Casas, "Improved tests of entanglement and Bell inequalities with LHC tops," [arXiv:2205.00542 [hep-ph]].
[16] Y. Afik and J. R. M. de Nova, "Quantum information with top quarks in QCD production," [arXiv:2203.05582 [quant-ph]].
[17] W. Gong, G. Parida, Z. Tu and R. Venugopalan, "Measurement of Bell-type inequalities and quantum entanglement from Λ-hyperon spin correlations at high energy colliders," [arXiv:2107.13007 [hep-ph]].
[18] A. J. Barr, "Testing Bell inequalities in Higgs boson decays," Phys. Lett. B **825**, 136866 (2022) [arXiv:2106.01377 [hep-ph]].
[19] A. J. Barr, P. Caban and J. Rembieliński, "Bell-type inequalities for systems of relativistic vector bosons," [arXiv:2204.11063 [quant-ph]].
[20] R. Aoude, E. Madge, F. Maltoni and L. Mantani, "Quantum SMEFT tomography: top quark pair production at the LHC," [arXiv:2203.05619 [hep-ph]].
[21] J. F. Clauser and A. Shimony, "Bell's theorem: Experimental tests and implications," Rept. Prog. Phys. **41**, 1881-1927 (1978);
J. F. Clauser, M. A. Horne, A. Shimony and R. A. Holt, "Proposed experiment to test local hidden variable theories," Phys. Rev. Lett. **23**, 880-884 (1969);
J. F. Clauser and M. A. Horne, "Experimental Consequences of Objective Local Theories," Phys. Rev. D **10**, 526 (1974).
[22] C. H. Bennett, D. P. DiVincenzo, J. A. Smolin and W. K. Wootters, "Mixed state entanglement and quantum error correction," Phys. Rev. A **54**, 3824-3851 (1996) [arXiv:quant-ph/9604024 [quant-ph]];
W. K. Wootters, "Entanglement of formation of an arbitrary state of two qubits," Phys. Rev. Lett. **80**, 2245-2248 (1998) [arXiv:quant-ph/9709029 [quant-ph]].
[23] J. S. Bell, "On the Einstein-Podolsky-Rosen paradox," Physics Physique Fizika **1**, 195-200 (1964).
[24] J. S. Bell, *Speakable and Unspeakable in Quantum Mechanics*, (Cambridge University Press, Cambridge, 1987-2004);
M. Redhead, *Incompleteness, Nonlocality and Realism*, (Clarendon Press, Oxford, 1987);
Quantum [Un]Speakables II: Half a Century of Bell's Theorem, R.A. Bertlmann and A. Zeilinger eds., (Springer, Berlin, 2017);
N. Brunner, D. Cavalcanti, S. Pironio, V. Scarani, and S. Wehner, "Bell nonlocality", Rev. Mod. Phys. **86** (2014) 419 [erratum: Rev. Mod. Phys. 86, 839 (2014)].
[25] R. Horodecki, P. Horodecki and M. Horodecki "Violating Bell inequality by mixed states: necessary and sufficient condition", Phys. Lett. **A200** (1995) 340.
[26] W. Bernreuther and Z. G. Si, "Top quark spin correlations and polarization at the LHC: standard model predictions and effects of anomalous top chromo moments," Phys. Lett. B **725**, 115-122 (2013) [erratum: Phys. Lett. B **744**, 413-413 (2015)] [arXiv:1305.2066 [hep-ph]].
[27] G. Mahlon and S. J. Parke, "Angular correlations in top quark pair production and decay at hadron colliders," Phys. Rev. D **53**, 4886-4896 (1996) [arXiv:hep-ph/9512264 [hep-ph]].
[28] W. Bernreuther, A. Brandenburg, Z. G. Si and P. Uwer, "Top quark spin correlations at hadron colliders: Predictions at next-to-leading order QCD," Phys. Rev. Lett. **87**, 242002 (2001) [arXiv:hep-ph/0107086 [hep-ph]];
W. Bernreuther, A. Brandenburg, Z. G. Si and P. Uwer, "Top quark pair production and decay at hadron colliders," Nucl. Phys. B **690**, 81-137 (2004) [arXiv:hep-ph/0403035 [hep-ph]].

[29] W. Bernreuther and Z. G. Si, "Distributions and correlations for top quark pair production and decay at the Tevatron and LHC.," Nucl. Phys. B **837**, 90-121 (2010) [arXiv:1003.3926 [hep-ph]].

[30] G. Mahlon and S. J. Parke, "Spin Correlation Effects in Top Quark Pair Production at the LHC," Phys. Rev. D **81**, 074024 (2010) [arXiv:1001.3422 [hep-ph]].

[31] W. Bernreuther, D. Heisler and Z. G. Si, "A set of top quark spin correlation and polarization observables for the LHC: Standard Model predictions and new physics contributions," JHEP **12**, 026 (2015) [arXiv:1508.05271 [hep-ph]].

[32] G. Aad *et al.* [ATLAS], "Observation of spin correlation in $t\bar{t}$ events from pp collisions at sqrt(s) = 7 TeV using the ATLAS detector," Phys. Rev. Lett. **108**, 212001 (2012) [arXiv:1203.4081 [hep-ex]];
"Measurement of Top Quark Polarization in Top-Antitop Events from Proton-Proton Collisions at $\sqrt{s} = 7$ TeV Using the ATLAS Detector," Phys. Rev. Lett. **111**, no.23, 232002 (2013) [arXiv:1307.6511 [hep-ex]];
S. Chatrchyan *et al.* [CMS], "Measurements of $t\bar{t}$ Spin Correlations and Top-Quark Polarization Using Dilepton Final States in *pp* Collisions at $\sqrt{s} = 7$ TeV," Phys. Rev. Lett. **112**, no.18, 182001 (2014) [arXiv:1311.3924 [hep-ex]];
G. Aad *et al.* [ATLAS], "Measurements of spin correlation in top-antitop quark events from proton-proton collisions at $\sqrt{s} = 7$ TeV using the ATLAS detector," Phys. Rev. D **90**, no.11, 112016 (2014) [arXiv:1407.4314 [hep-ex]].

[33] G. Aad *et al.* [ATLAS], "Measurement of Spin Correlation in Top-Antitop Quark Events and Search for Top Squark Pair Production in pp Collisions at $\sqrt{s} = 8$ TeV Using the ATLAS Detector," Phys. Rev. Lett. **114**, no.14, 142001 (2015) [arXiv:1412.4742 [hep-ex]];
M. Aaboud *et al.* [ATLAS], "Measurements of top quark spin observables in $t\bar{t}$ events using dilepton final states in $\sqrt{s} = 8$ TeV pp collisions with the ATLAS detector," JHEP **03**, 113 (2017) [arXiv:1612.07004 [hep-ex]].

[34] A. M. Sirunyan *et al.* [CMS], "Measurement of the top quark polarization and $t\bar{t}$ spin correlations using dilepton final states in proton-proton collisions at $\sqrt{s} = 13$ TeV," Phys. Rev. D **100**, no.7, 072002 (2019) [arXiv:1907.03729 [hep-ex]].

[35] R. D. Ball *et al.* [PDF4LHC Working Group], J. Phys. G **49**, no.8, 080501 (2022) [arXiv:2203.05506 [hep-ph]].

[36] J. Alwall, R. Frederix, S. Frixione, V. Hirschi, F. Maltoni, O. Mattelaer, H. S. Shao, T. Stelzer, P. Torrielli and M. Zaro, "The automated computation of tree-level and next-to-leading order differential cross sections, and their matching to parton shower simulations," JHEP **07**, 079 (2014) [arXiv:1405.0301 [hep-ph]].

[37] M. Czakon, A. Mitov and R. Poncelet, "NNLO QCD corrections to leptonic observables in top-quark pair production and decay," JHEP **05**, 212 (2021) [arXiv:2008.11133 [hep-ph]].

[38] M. Czakon, D. Heymes and A. Mitov, "High-precision differential predictions for top-quark pairs at the LHC," Phys. Rev. Lett. **116**, no.8, 082003 (2016) [arXiv:1511.00549 [hep-ph]];
R. Frederix, I. Tsinikos and T. Vitos, "Probing the spin correlations of $t\bar{t}$ production at NLO QCD+EW," Eur. Phys. J. C **81**, no.9, 817 (2021) [arXiv:2105.11478 [hep-ph]];
A. Cakir and O. Kolay, "Comparison of spin-correlation and polarization variables of spin density matrix for top quark pairs at the LHC and New Physics implications," [arXiv:2201.06107 [hep-ph]].

[39] B. Lillie, J. Shu and T. M. P. Tait, "Top Compositeness at the Tevatron and LHC," JHEP **0804**, 087 (2008) [arXiv:0712.3057 [hep-ph]];
K. Kumar, T. M. P. Tait and R. Vega-Morales, "Manifestations of Top Compositeness at Colliders," JHEP **0905**, 022 (2009) [arXiv:0901.3808 [hep-ph]];
Z. Hioki and K. Ohkuma, "Search for anomalous top-gluon couplings at LHC revisited," Eur. Phys. J. C **65**, 127 (2010) [arXiv:0910.3049 [hep-ph]] ;
C. Degrande, J. -M. Gerard, C. Grojean, F. Maltoni and G. Servant, "Non-resonant New Physics in Top Pair Production at Hadron Colliders," JHEP **1103**, 125 (2011) [arXiv:1010.6304 [hep-ph]];
D. Choudhury and P. Saha, "Probing Top Anomalous Couplings at the Tevatron and the Large Hadron Collider," Pramana **77**, 1079 (2011) [arXiv:0911.5016 [hep-ph]];
S. S. Biswal, S. D. Rindani and P. Sharma, J. F. Kamenik, M. Papucci and A. Weiler, "Constraining the dipole moments of the top quark," Phys. Rev. D **85**, 071501 (2012) [arXiv:1107.3143 [hep-ph]];
S. S. Biswal, S. D. Rindani and P. Sharma, "Probing chromomagnetic and chromoelectric couplings of the top quark using its polarization in pair production at hadron colliders," Phys. Rev. D **88**, 074018 (2013) [arXiv:1211.4075 [hep-ph]];
Z. Hioki and K. Ohkuma, "Latest constraint on non-standard top-gluon couplings at hadron colliders and its future prospect," [arXiv:1306.5387 [hep-ph]];
C. Englert, A. Freitas, M. Spira and P. M. Zerwas, "Constraining the Intrinsic Structure of Top-Quarks," Phys. Lett. B **721**, 261 (2013) [arXiv:1210.2570 [hep-ph]];
M. Fabbrichesi, M. Pinamonti and A. Tonero, "Limits on anomalous top quark gauge couplings from Tevatron and LHC data," Eur. Phys. J. C **74**, no.12, 3193 (2014) [arXiv:1406.5393 [hep-ph]];
D. Barducci, M. Fabbrichesi and A. Tonero, "Constraints on top quark nonstandard interactions from Higgs and $t\bar{t}$ production cross sections," Phys. Rev. D **96**, no.7, 075022 (2017) [arXiv:1704.05478 [hep-ph]].

[40] A. M. Sirunyan *et al.* [CMS], "Measurement of the top quark forward-backward production asymmetry and the anomalous chromoelectric and chromomagnetic moments in pp collisions at $\sqrt{s} = 13$ TeV," JHEP **06**, 146 (2020) [arXiv:1912.09540 [hep-ex]].

[41] I. Brivio, S. Bruggisser, F. Maltoni, R. Moutafis, T. Plehn, E. Vryonidou, S. Westhoff and C. Zhang, "O new physics, where art thou? A global search in the top sector," JHEP **02**, 131 (2020) [arXiv:1910.03606 [hep-ph]];
J. J. Ethier *et al.* [SMEFiT], "Combined SMEFT interpretation of Higgs, diboson, and top quark data from the LHC," JHEP **11**, 089 (2021) [arXiv:2105.00006 [hep-ph]].

[42] C. Severi and E. Vryonidou, 'Quantum entanglement and top spin correlations in SMEFT at higher orders," [arXiv:2210.09330 [hep-ph]].

[43] M. Grazzini, S. Kallweit and M. Wiesemann, Eur. Phys. J. C **78**, no.7, 537 (2018) [arXiv:1711.06631 [hep-ph]].

[44] M. Aaboud *et al.* [ATLAS], "Search for new phenomena in dijet events using 37 fb^{-1} of pp collision data collected at $\sqrt{s}$ =13 TeV with the ATLAS detector," Phys. Rev. D **96**, no.5, 052004 (2017) [arXiv:1703.09127 [hep-ex]].

[45] A. M. Sirunyan *et al.* [CMS], "Search for new physics in dijet angular distributions using proton–proton collisions at $\sqrt{s}$ = 13 TeV and constraints on dark matter and other models," Eur. Phys. J. C **78**, no.9, 789 (2018) [erratum: Eur. Phys. J. C **82**, no.4, 379 (2022)] [arXiv:1803.08030 [hep-ex]].

[46] R. L. Workman *et al.* [Particle Data Group], "Review of Particle Physics," PTEP **2022**, 083C01 (2022).

[47] B. K. Bullock, K. Hagiwara and A. D. Martin, Nucl. Phys. B **395** (1993) 499.

[48] M. Bonvini, S. Marzani, C. Muselli and L. Rottoli, "On the Higgs cross section at N^3LO+N^3LL and its uncertainty," JHEP **08**, 105 (2016) [arXiv:1603.08000 [hep-ph]].

[49] K. Desch, A. Imhof, Z. Was and M. Worek, "Probing the CP nature of the Higgs boson at linear colliders with tau spin correlations: The Case of mixed scalar - pseudoscalar couplings," Phys. Lett. B **579**, 157-164 (2004) [arXiv:hep-ph/0307331 [hep-ph]].

[50] A. Rouge, "CP violation in a light Higgs boson decay from tau-spin correlations at a linear collider," Phys. Lett. B **619**, 43-49 (2005) [arXiv:hep-ex/0505014 [hep-ex]].

[51] S. Berge, W. Bernreuther and S. Kirchner, "Determination of the Higgs CP-mixing angle in the tau decay channels at the LHC including the Drell–Yan background," Eur. Phys. J. C **74**, no.11, 3164 (2014) [arXiv:1408.0798 [hep-ph]].

[52] W. Bernreuther, M. Flesch and P. Haberl, "Signatures of Higgs bosons in the top quark decay channel at hadron colliders," Phys. Rev. D **58**, 114031 (1998) [arXiv:hep-ph/9709284 [hep-ph]].

[53] A. V. Gritsan, R. K. Barman, I. Bozovic-Jelisavcic, J. Davis, W. Dekens, Y. Gao, D. Goncalves, L. S. M. Guerra, D. Jeans and K. Kong, *et al.* "Snowmass White Paper: Prospects of CP-violation measurements with the Higgs boson at future experiments," [arXiv:2205.07715 [hep-ex]].

[54] V. L. Lyuboshitz and V. V. Lyuboshitz, "On the correlations of polarizations in the system of two photons," AIP Conf. Proc. **915**, no.1, 268-271 (2007).

[55] M. May, "On the Polarization of High Energy Bremsstrahlung and of High Energy Pairs," Phys. Rev. 84 (1951) 265.

[56] A. Borsellino, "Momentum Transfer and Angle of Divergence of Pairs Produced by Photons," Phys. Rev. **89**, 1023-1025 (1953).

[57] V. F. Boldyshev, E. A. Vinokurov, N. P. Merenkov and Y. P. Peresunko, "Measurement of photon beam linear polarization using asymmetry of the recoil electrons from the photoproduction of e+ e- pairs on electrons," Phys. Part. Nucl. **25**, 292-331 (1994).

[58] G. Barbiellini, G. Depaola and F. Longo, "Measuring polarization of high-energy gamma rays," Nucl. Instrum. Meth. A **518**, 195-197 (2004);
G. O. Depaola and M. L. Iparraguirre, "Angular distribution for the electron recoil in pair production by linearly polarized gamma-rays on electrons," Nucl. Instrum. Meth. A **611**, 84-92 (2009);
M. L. Iparraguirre and G. O. Depaola, "Pair production by gamma-rays on electrons. Threshold for the momentum recoil detection," Eur. Phys. J. C **71**, 1778 (2011).

[59] D. Bernard [HARPO], "Polarimetry of cosmic gamma-ray sources above e^+e^- pair creation threshold," Nucl. Instrum. Meth. A **729**, 765-780 (2013) [arXiv:1307.3892 [astro-ph.IM]].

[60] S. Agostinelli *et al.* [GEANT4], "GEANT4–a simulation toolkit," Nucl. Instrum. Meth. A **506**, 250-303 (2003).

[61] D. Bernard, "γ-ray polarimetry with conversions to e^+e^- pairs: polarization asymmetry and the way to measure it," Astropart. Phys. 88 (2017) 30.

[62] W. Bernreuther and A. Brandenburg, "Tracing CP violation in the production of top quark pairs by multiple TeV proton proton collisions," Phys. Rev. D **49**, 4481-4492 (1994) [arXiv:hep-ph/9312210 [hep-ph]].

[63] P. Uwer, "Maximizing the spin correlation of top quark pairs produced at the Large Hadron Collider," Phys. Lett. B **609**, 271-276 (2005) [arXiv:hep-ph/0412097 [hep-ph]].